POLYTECHNIQUE MONTRÉAL

affiliée à l'Université de Montréal

An Investigation of Tibial Spike Instability in Total Knee Replacement with iAssist Technology

ASRA SALEH

Institut de génie biomédical

Mémoire présenté en vue de l'obtention du diplôme de *Maîtrise ès sciences appliquées*

Génie biomédical

Avril 2022

POLYTECHNIQUE MONTRÉAL

Affiliée à l'Université de Montréal

Ce mémoire intitulé :

An Investigation of Tibial Spike Instability in Total Knee Replacement with iAssist Technology

présenté par Asra SALEH

en vue de l'obtention du diplôme de *Maîtrise ès sciences appliquées*

a été dûment accepté par le jury d'examen constitué de :

L'Hocine YAHIA, président

Delphine PÉRIÉ-CURNIER , membre et directrice de recherche

Maxime RAISON, membre

DEDICATION

To my beloved family, Pouyan and Rasta!

ACKNOWLEDGEMENTS

I would like to thank my master's supervisor professor Delphine Périé-Curnier for inspiring me to go forward with this project. I would never have been able to finish my thesis without her outstanding advice and guidance.

I would also like to thank all my co-workers at Zimmer Biomet for their teamwork. My special thanks go to Emmanuel Gaillard, Joseph Madier-Vigneux, Caroline Ceccaldi, Nathalie Godin, and Benoit Waeckel, who patiently and tirelessly supported me in attempting to understand the complexities of working on DHFs. I would not have been able to understand or carry out the verification/validation process without their significant contributions. Also, all the members of the iASSIST team for allowing me to be a part of your lab and work with you.

I am extremely grateful to my husband and my daughter for their love, understanding, prayers, and continuing support to complete this research work. Finally, I would like to thank my family and friends for supporting me through it all.

This work was funded by the Canadian Network of Centres of Excellence, Mitacs.

RÉSUMÉ

L'arthroplastie du genou est une chirurgie de remplacement articulaire qui nécessite l'ablation des surfaces endommagées ou blessées du fémur, du tibia et de la rotule pour les remplacer par des implants métalliques. Le succès de l'arthroplastie totale de genou dépend de la précision des résections osseuses et d'un bon alignement du genou. Divers systèmes de chirurgie assistée par ordinateur (CAS) ont été améliorés pour atteindre cet objectif, mais la complexité de ces systèmes les a empêchés d'être utilisés à grande échelle. Entre-temps, un système de navigation basé sur des accéléromètres a été développé, iASSIST, qui combine la précision des systèmes CAS avec des procédures d'alignement conventionnelles. La stabilité de la pointe insérée dans l'os est essentielle pour la précision du système. À la suite de cette nécessité, ce projet de maitrise est défini pour caractériser l'instabilité de l'instrument de référence tibial le plus récent d'iASSIST.

La conception précédente de l'instrument Tibial Alignment Guide utilisé dans l'iAssist Knee présentait un risque d'interférence de broche entre la longue pointe de la référence tibiale et les broches à insérer dans le guide de coupe. Ce problème a conduit à la refonte de la Tibial Reference originale avec deux spikes avec le nouveau design pour Tibial Reference contenant une seule spike. En ce qui concerne les exigences réglementaires en matière de contrôle de la conception, décrites du code des règlements fédéraux, les règlements sur le contrôle de la conception doivent s'appliquer à la conception et au développement de ce nouveau produit pour s'assurer que les exigences de conception spécifiées sont respectées.

Cette nouvelle référence tibiale contient un nouvel instrument et une nouvelle technique chirurgicale avec une pointe qui sera insérée dans le tibia. Pour que le système soit précis, la référence tibiale doit être stable dans l'os. Par conséquent, la stabilité de cet instrument est un facteur qui doit être caractérisé lorsqu'il est impacté dans l'os. Suite à cette nécessité, ce projet de maître vise à caractériser l'instabilité de l'instrument de référence tibial le plus récent d'iASSIST. En outre, les erreurs causées par l'instabilité de l'insertion du pic de référence tibial dans l'os ont été étudiées.

Dans ce projet, le bras CMM aide à calculer toutes les mesures liées à la rotation (en termes de rotation, de varus/valgus et de pente tibiale par rapport à l'axe mécanique du tibia) et à la translation entre l'os et la référence tibiale à plusieurs points clés de la chirurgie. De plus, une validation de la méthode d'essai a été effectuée pour la méthode d'essai de caractérisation de l'instabilité afin d'évaluer la répétabilité et la reproductibilité des mesures de la CMM. La somme résiduelle des carrés (RSS) de la référence tibiale et les variations osseuses (en Varus/Valgus, Flexion/Extension et Rotation) sont considérées comme l'erreur de mesure.

Enfin, l'analyse de répétabilité et de reproductibilité de la jauge (Gage R&R) a été appliquée pour quantifier l'erreur de mesure. En traitant les expériences et en analysant les résultats, la principale source de variation a été détectée et la cause profonde de ces mesures erronées a été trouvée. Les résultats de la reproductibilité ont pu déterminer que les opérateurs étaient une source importante de variation qui avait une incidence sur la variabilité du système de mesure. En outre, la grande quantité de répétabilité montre qu'une grande partie de la variation totale était liée à l'instrument de mesure. Les recommandations pour résoudre ces problèmes sont probablement l'application des CMM sans contact qui fournissent les mesures les plus précises ainsi que la mise en œuvre d'opérateurs formés pour travailler avec la CMM. Par conséquent, il serait pertinent de mener d'autres études pour corriger les mesures erronées et améliorer les performances du système de mesure problématique.

Abstract

Total knee arthroplasty (TKA) is a joint replacement surgery that requires the removal of the damaged or injured surfaces of the femur, tibia, and patella to replace with metallic or plastic implants. Successful Total knee arthroplasty depends on the accuracy of bone resections and proper knee alignment. Various computer-assisted surgery (CAS) systems have been improved to achieve this aim, but the complexity of these systems has prevented them from being widely used. Meanwhile, a navigation system based on accelerometers has been developed, such as the iASSIST knee, which combines the precision of large-console CAS systems with the ease of conventional alignment procedures by avoiding the preoperative imaging and eliminating large console required for registration. The stability of the spike inserted into the bone is critical for the accuracy of the system.

The previous design of the Tibial Alignment Guide instrument used in the iASSIST Knee had a risk of pin interference between the long spike of the Tibial Reference (TR) and the pins to be inserted in the Cut Guide. This issue led to the redesign of the original TR with two spikes with the new design for TR containing a single spike. Regards to regulatory requirements of design controls, outlined by Food and Drug Administration, design control regulations must apply to the design and development of this new product to ensure that specified design requirements are met.

This newly designed Tibial Reference contains a new instrument and new surgical technique with a spike that will be inserted into the tibia. For the system to be accurate, the Tibial Reference needs to be stable in the bone. Therefore, the stability of this instrument is a factor that should be characterized when impacted into the bone. Following this necessity, this master project aims to characterize the instability of the most recent Tibial Reference instrument of iASSIST. In addition, errors caused by the instability of the insertion of the Tibial Reference spike into the bone have been investigated.

In this project, the CMM arm helps to calculate all the measurements related to the rotation (in terms of rotation, varus/valgus, and tibial slope in relation with the tibia mechanical axis) and translation between the bone and the Tibial Reference at multiple key points during the surgical

flow. Furthermore, a test method validation was conducted to the instability characterization test method to assess the repeatability and reproducibility of the CMM measurements. The Residual Sum of Squares (RSS) of the Tibial Reference and bone variations (in Varus/Valgus, Flexion/Extension, and Rotation) are considered as the measurement error.

Finally, the gage repeatability and reproducibility (Gage R&R) analysis were applied to quantify the measurement error. Through processing the experiments and analyzing the results, the major source of variation was detected, and the root cause of these erroneous measurements was found. The results from Reproducibility could determine that the operators were a significant source of variation that impacted the variability of the measurement system. In addition, the great amount of Repeatability shows that a major part of the total variation was related to the gage instrument. Recommendations to solve these issues are the application of the non-contact CMMs which provide the most accurate measurements along with implementing trained operators for working with CMM. Therefore, it would be relevant to carry out further studies to correct the erroneous measurements and improve the problematic measurement system’s performance.

TABLE OF CONTENTS

LIST OF TABLES

LIST OF FIGURES

LIST OF SYMBOLS AND ABBREVIATIONS

AOANJRR Australian Orthopaedic Association National Joint Replacement Registry

AACMMs Articulated Arm Coordinate Measuring Machines

ACL anterior cruciate ligament

CAS Computer-assisted surgery

CT computerized tomography

CMM Coordinate Measuring Machines

EM extramedullary alignment

G1 Goal 1

G2 Goal 2

IM intramedullary alignment

MRI Magnetic resonance imaging

OA Osteoarthritis

PCL posterior cruciate ligament

TKA Total Knee Arthroplasty

TR Tibial Reference

LCL Lower control limit

UCL Upper control limit

CHAPTER 1 INTRODUCTION

Osteoarthritis (OA) is one of the most common degenerative diseases that cause joint function loss and significant pain (Zhang & Jordan, 2010). According to the World Health Organization, OA was the tenth largest cause of disability-adjusted life years (2.5%) in high-income nations by 2015. The overall yearly cost of OA in the UK economy is reported to be £12 billion and $185.5 billion for the US (Mathers & Loncar, 2006). Moreover, Hip and Knee replacement with over 138,000 surgeries (75,073 knee replacements in 2019-2020) performed annually and yearly inpatient expenses of more than $1.4 billion, are continued to be two of the most common surgeries in Canada (Blankstein et al., 2021) (*National Joint Replacement Registry AOA Hip*, 2021).

One of the reliable surgeries that provide significant outcomes for patients suffering from knee joint diseases is Total Knee Arthroplasty (TKA). However, TKA revision procedures cost the US economy $2.7 billion each year, with forecasts indicating that this cost will rise to $13 billion by 2030 (Concoff et al., 2021). To minimize revision surgeries in TKA, Computer-assisted surgery (CAS) has been improved to enhance the precision of bone preparation and component alignment during surgery preoperatively or intraoperatively. The rate of CAS navigation has grown from 2.4 percent in 2003 to 33.2 percent in 2018, according to the Australian Orthopaedic Association National Joint Replacement Registry (AOANJRR) ("National Joint Replacement Registry AOA Hip, Knee & Shoulder Arthroplasty ", 2020).

One of these computers assisted surgical instrument system is the iASSIST knee system. The navigation system of iASSIST is designed based on using disposable electronic pods which are attached to the femoral and tibial resection instruments (Kinney et al., 2018). This intelligent cutting block system offers intraoperative verification for both stages of surgery, bone cuts and overall alignment, which improves postoperative functional outcome (Li et al., 2019).

The main goal of this master's project is to validate the stability of the new instrument designed for iASSIST to make sure the system is accurate during the surgery (G1). To this end, it is first required to characterize the error caused by the instability of the insertion of the Tibial Reference spike into the bone, with aim of using the result of the test as an error value in the system stack-up (G.1.1). Moreover, it requires identifying which step of the surgery caused the most

movement of the Tibial Reference (G.1.2). Once the instability characterization was performed, the method used for this characterization must be validated for producing valid results (G2).

This introduction is followed by six other chapters. Chapter 2 presents the literature review about the research project. Chapter 3 outlines the objectives of this study. Chapter 4 explains the materials and methods used for this project. In this chapter, the method of instability error measurement by the CMM machine is introduced and the error of the system is calculated. Chapter 5 consists of the test method validation used in chapter 3. Chapter 6 discusses the Gage R&R study. Chapter 7 concludes this master's project and suggests some ideas of the alternative methods of the measurement system.

CHAPTER 2 LITERATURE REVIEW

2.1 Knee Anatomy

The knee joint is the largest hinge joint in the human body which allows movement like flexion and extension in the sagittal plane, and varus and valgus rotation in the frontal plane (Whitesides, 2001). There are two articulations in the knee joint: the tibiofemoral and patellofemoral. The tibiofemoral joint is known as a weight-bearing joint that connects the proximal tibia to the distal femur, and the main motion of this articular is flexion and extension. The patellofemoral joint is constructed from a network of bones, muscles, and cartilages which are function as a stabilizer to reduce frictional stresses on the femoral condyles. The femorotibial and patellofemoral joints provide flexion and extension motions in the sagittal plane and internal and external rotation in the transverse plane, and the varus and valgus occur in the frontal plane (Abulhasan et al., 2017). Knee stability and function are mostly controlled by the anterior cruciate ligament (ACL) and the posterior cruciate ligament (PCL) (Fig 2.1). These two main ligaments that cross within the knee joint, control flexion and extension without sliding back and forth. The ACL keeps the tibia from moving forward along the femur, whereas the PCL keeps the tibia and femur from moving backward ((Younger et al., 2016), (Edwards et al., 2007)).

The knee joint is more prone to injury than any other joint in the body due to its location between the body's two longest lever arms, the femur and tibia, and its role in weight bearing. Many forces on the knee joint can affect the articulating surfaces of the knee and destroy the articular cartilage. In severe cases of damaged knee like osteoarthritis or rheumatoid arthritis the joint is usually considered to be treated with a total knee replacement surgery or total knee arthroplasty (TKA) (Abulhasan et al., 2017).

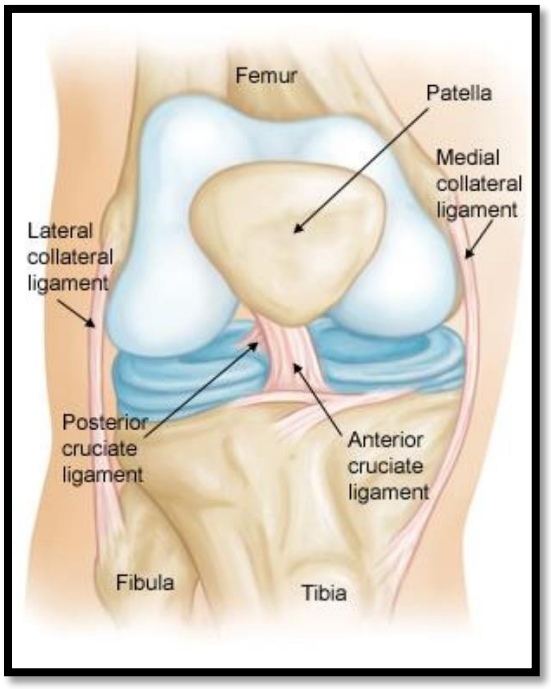

Figure 2.1. Normal knee anatomy. (Arthritis of the Knee - OrthoInfo - AAOS) (Surgeons, 2021).

2.2 Knee Osteoarthritis

Arthritis is a term used to describe any condition that causes pain and inflammation in the joints (Fig. 2.2). The most common types of arthritis are osteoarthritis and rheumatoid arthritis. Osteoarthritis includes symptoms of joint pain, stiffness, tenderness, decreased function and disability.

Arthritis is the most often reported long-term health condition in Canada, with over 6 million Canadians, which is about 20% of the Canadian population. The number of people living with arthritis is expected to rise approximately 8.8 million in 2040 (E. Badley et al., 2019).

Treatment options for conservative knee osteoarthritis contains physiotherapy, pharmaceutical agents, injections, and Cannabis products. In case conservative procedures are infeasible, a joint replacement may be necessary. Arthroplasty is a procedure that realigns or reconstructs a joint to reduce discomfort and restore range of motion. Arthroplasty can be performed on a portion of the joint, or the total joint can be replaced (Feeley et al., 2010).

2.3 Total Knee Arthroplasty

The knee is the most frequent joint to develop OA, which affects the articulating surfaces of the knee and causes articular cartilage degradation. For treatment of chronic degenerative like rheumatoid arthritis, the joint is usually replaced with an artificial material (E. D. Badley, M., 2003).

TKA is a Joint replacement surgery in which the damaged or injured surfaces of the femur, tibia and patella is replaced with metallic or plastic implants. However, the anterior cruciate ligament (ACL) is usually sacrificed during TKA surgery, new advantages in implant fixation like cruciate retaining implants help to preserve the posterior cruciate ligament (PCL). Both the medial and lateral collateral ligaments are left intact (Parcells & Tria Jr, 2016).

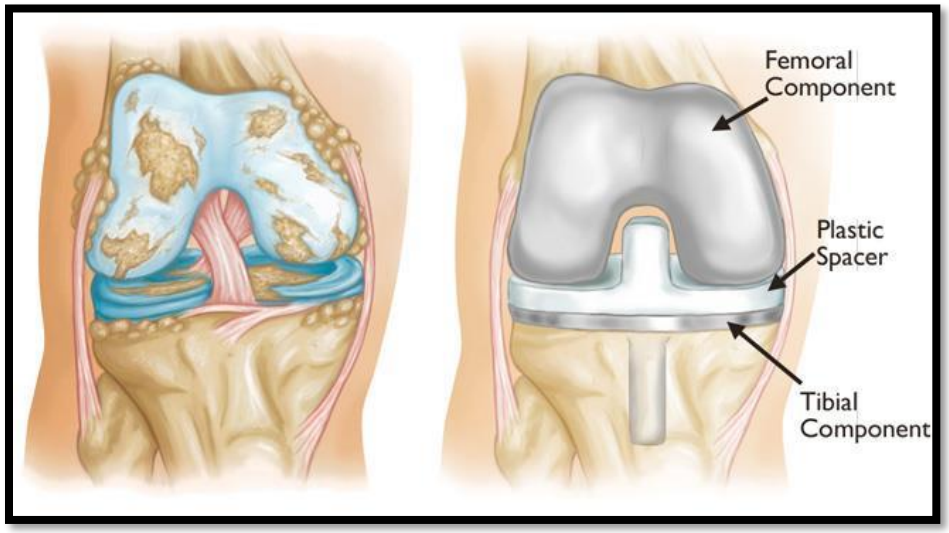

Figure 2.2 Severe osteoarthritis (left). Total knee replacement (right) (Surgeons, 2021).

2.4 Knee alignment

The knee alignment is a key factor of load distribution at knee joint. Any change in hip-knee-ankle alignment from neutral or collinear influences load distribution at the knee and decrease the knee function. In the healthy joint, the load-bearing axis is a straight line which runs from hip, passes from mid femoral head, and ends to mid ankle. In mal-aligned knee like valgus knee,

cartilage damage induces deformity in the knee and abnormal force is applied to a certain area of the knee (Iseki et al., 2009).

One of the most common deformities of alignment is Bow leg which is also known as genu varum. It is commonly seen in conditions of severe degree osteoarthritis of the knee in which the alignment is severely disrupted. The goal of TKA surgery for these diseases are restoring the alignment (Azar et al., 2020; JC, 2010).

Typically, alignment of the lower extremity is in 3° valgus of the vertical line of the body. In femur, the vertical axis is defined as a line perpendicular to the ground, and mechanical axis is a line from the center of the femoral head to the center of trochlea. The anatomic axis is a line collinear with the shaft of femur. On average, there is a 6° difference between the anatomic axis and mechanical axis of the femur, and about 9° difference between the anatomic axis of the femur with the vertical axis of the body. The knee anatomic angle which is also known as tibiofemoral angle is about 6° valgus (Azar et al., 2020).

In tibia, mechanical axis is defined as a line runs from typical plateau to the center of the tibial plafond, and anatomic axis is a co-linear to the center of the shaft. The tibia has a mechanical axis that matches the anatomical axis, and the relationship between the mechanical axis and the anatomic axis in tibia is about 3° with the articular surface of the proximal tibia (Kang et al., 2018). Anatomical axis of tibia is 3° varus from vertical axis of body. Fig. 2.3 illustrates the summery of these angles (Azar et al., 2020).

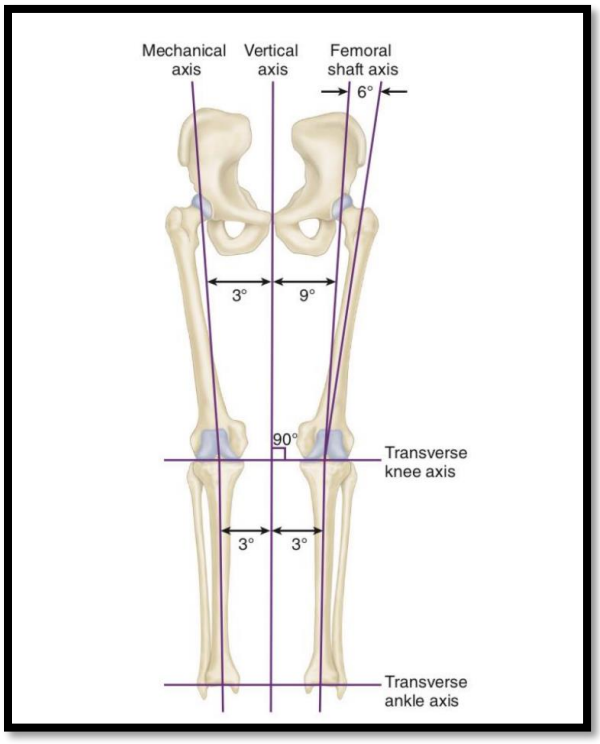

Figure 2.3 The mechanical and anatomic axis of the lower extremity (Azar et al., 2020).

A full-leg standing digital radiography which is also called a 3-foot standing x-ray or hip-to-ankle x-ray helps to calculate the alignment values of patients in preoperative planning of TKA. These preoperative measurements aids in the restoration of the lower limb alignment and knee alignment measurements. To indicate an overall alignment of the leg, the mechanical axis of the lower extremity is used. While the neutral mechanical axis passes the center of the knee, any medial deviation from the mechanical axis counts the limb in varus. However, in valgus knee, the mechanical axis line goes across the lateral compartment (Whitaker & Vuillermin, 2016).

The concept of physiologic varus has recently gained popularity. It is described as a 3° or greater varus alignment of the lower limbs. Bellemans et al. stated that in a general healthy population "32% of men and 17% of women had constitutional varus knees with a natural mechanical alignment of 3° varus or more" (Johan Bellemans et al., 2012). Another study by Vanlommel et al. indicates that the percentages of physiologic varus within patients with medial OA varies as 46% in men and 23% of women (Lanting et al., 2018; Vandekerckhove et al., 2017).

In TKA, the goal is to restore the normal anatomical alignment of the knee in the coronal and sagittal plane. The coronal alignment can be calculated by measuring the angle between mechanical axis of femur and tibia in the varus or valgus state. Another important definition for balancing a TKA appropriately, is the sagittal alignment of the knee to prevent the knee from falling into recurvatum (Luo et al., 2020).

2.5 Surgical alignment technique

Total knee arthroplasty (TKA) is one of the successful procedures to battle the deformity caused by arthritis. The primary goal of TKA is to restore knee stability by increasing range of motion while also removing pain. These goals can be fulfilled by proper implant alignment and soft tissue balancing (Neil P Sheth et al., 2017). There are several alignment techniques that have been suggested, like: Mechanical alignment, Kinematic alignment, Anatomic Alignment, adjusted Mechanical alignment, and Restricted Kinematic alignment. Mechanical and kinematic alignment will be the emphasis of this thesis.

2.5.1 Mechanical alignment technique for TKA

The mechanical alignment technique was first introduced by Michael Freeman (Freeman et al., 1973), 50 years ago for femoral and tibial bone cuts in total knee arthroplasty (TKA). The original idea behind bone incisions in mechanical alignment was to keep the joint line aligned to the limb's neutral mechanical axis. It contains an initial femoral cut which is perpendicular to the mechanical axis of the femur, and the tibial resection performs perpendicular to the mechanical axis of the tibia. The outcome is a knee that is generally positioned around 4°–5° valgus, however this might vary depending on the patient's height and limb morphology. Regarding to balance flexion and extension gaps, femoral component positioning is performed at 3° of external rotation (John N Insall et al., 1985).

The goal was to disperse the load more evenly over the tibial compartments to minimize the adduction moment. This approach leads to create a biomechanically friendly prosthetic knee that helps to avoid instability, rapid polyethylene wear, and early implant loosening (Sharkey et al., 2002). Although mechanically alignment technique has been significantly improved, functionally outcomes remained disappointing by ignoring other parameters like individual native knee anatomy and physiological soft tissue laxities (Le et al., 2014). It has been reported that 10- 20% patient dissatisfaction (D. Nam et al., 2014) is due to stiffness, swelling, pain and instability

symptoms which are not improved even with computer assisted surgery (CAS) and robotic surgery. This is most likely due to the inability to restore patient-specific knee kinematics (Dennis et al., 2004).

2.5.2 Kinematic alignment technique

Knee kinematics is a significant aspect that influences pain, function, satisfaction, and revision. Knee kinematics after TKA can be influenced by a variety of factors, including implant design, component placement, and soft tissue tensions (Matsuzaki et al., 2014). There are lots of debates due to undesirable kinematic effects of positioning the components mechanically. Changing the ligaments tension results in higher stress on the altered joint, and this might be the source of pain during knee motion (Schiraldi et al., 2016).

There are differences in the principle of component placement for two surgical procedures of mechanical alignment and kinematic alignment techniques. Mechanical alignment places the components perpendicular to the vertical mechanical axis while kinematic alignment, places the components parallel to the transverse flexion extension axis which follows the inclination of the natural joint line. The kinematic alignment, the best-fitting femoral component's transverse axis matches with the femur's main transverse axis, around which the tibia flexes and extends. The surgeon releases ligaments to balance the knee in mechanical alignment, while the kinematic alignment seeks to restore the joint line to the individual patient pre-disease state, referencing the flexion-extension axis (Schiraldi et al., 2016). The kinematic alignment is mainly a bone treatment in which ligaments are spared, and they release in only necessary circumstances. The goal is to have components that are completely anatomically positioned on the resurfaced bone (Howell & Hull, 2014).

2.6 Knee Arthroplasty Techniques

2.6.1 Soft Tissue Techniques

Symmetric and equal flexion and extension gaps are key components to accomplish ligament and soft tissue balancing. Many reported issues after TKA surgery such as stiffness, pain, instability,

limited flexion, abnormal kinematics, and accelerated polyethylene wear have resulted from inadequate correction of soft tissue balancing (Daines & Dennis, 2014).

Measured resection and gap balancing are two main surgical techniques for successful total knee arthroplasty, in which, joint laxity and over tension issues are addressed. In the measured resection technique, bone resections and ligament release are applied to match the prosthesis thickness to restore the joint line for proper function. To reach a precise bone cut, the surgeon uses jigs to measure the amount of bone that should be removed to be matched with cruciate-retaining implants (Fig. 2.4). This implant is suitable for patients with a healthy PCL, and the anterior cruciate ligament (ACL) is removed (Tapasvi et al., 2020).

Figure 2.4 Johnson and Johnson ATTUNE® Cementless, cruciate retaining femoral implant ("THE ATTUNE CEMENTLESs KNEE SYSTEM,").

Gap balancing aims to achieve optimal flexion and extension gap symmetry, and this technique is developed for posterior cruciate ligament **(**PCL) substituting implants (Fig. 2.5) (John N. Insall, 1993). Gap balancing is achieved by obtaining symmetric ligament tension in extension and then adjusting femoral implant rotation based on a symmetric flexion gap (N. P. Sheth et al., 2017)

Figure 2.5 Zimmer NexGen LPS Flex cruciate (biomet, 2016).

2.6.2 Patient Specific Knee Arthroplasty

In patient-specific knee replacement method, radiograph, and magnetic resonance imaging (MRI) are used to generate a preoperative three-dimensional (3D) model of the bone. These 3D models able the surgeon to choose the optimal implant for the patient, and plan bone resection regions based on the patient's landmarks. The approved preoperative plans are used to manufacture disposable and customized prototypes of cutting guides (Fig. 2.6) (Denis Nam et al., 2012).

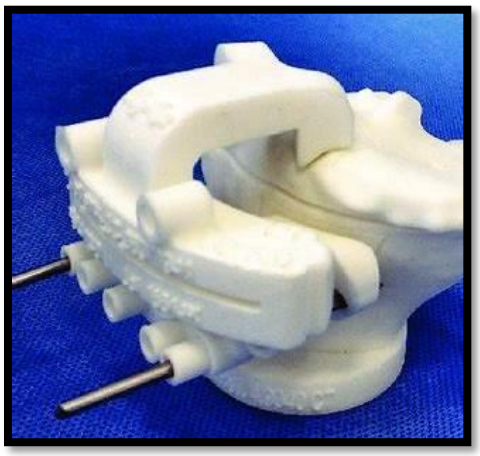

Figure 2.6 Disposal patient specific cutting guide placed on 3D printed model of patient's bone (Mattei et al., 2016).

2.7 TKA revision causes

Among the reasons that cause arthroplasty failure, aseptic loosening and malalignment are major concerns. It has been reported that many early implant failures are related to knees alignment in greater than 3° varus or valgus. The goal of proper alignment can be achieved by bone resection precisely and accurate implant placement. Proper alignment of the knee improves the long-term outcomes of postoperative surgery, and it decreases the stresses on bone/prosthesis interfaces. To attain this goal, various technologies like computer navigation surgery (CAS) have been established to help the surgeon to restore the patient's lower extremity to neutral. (Quack et al., 2012)

2.8 Surgical Navigation

Implant function is highly affected by implant alignment. The surgical technique and implant design can prevent femoral condylar lift-off and other abnormal knee function. Component malalignment can be restricted by following cutting guides and performing resections on the bone base on the landmarks. The first principle to create resections on the bone is identifying the landmarks (John N. Insall et al., 2002).

2.8.1 Landmarks

In the normal knee, the mechanical axis that supports the bodyweight is passing through the knee. In the valgus knee a lateral shift and, in the varus knee a medial shift, change the stress distribution in the knee which can be resulted in uneven joint loading (Fig. 2.7). For instrument placement, the intramedullary canal of the tibia or femur (base on the anatomical axis) is used as reference landmarks. These landmarks indicate the angle between the anatomical and mechanical axis to resect the knee (John N. Insall, 1993).

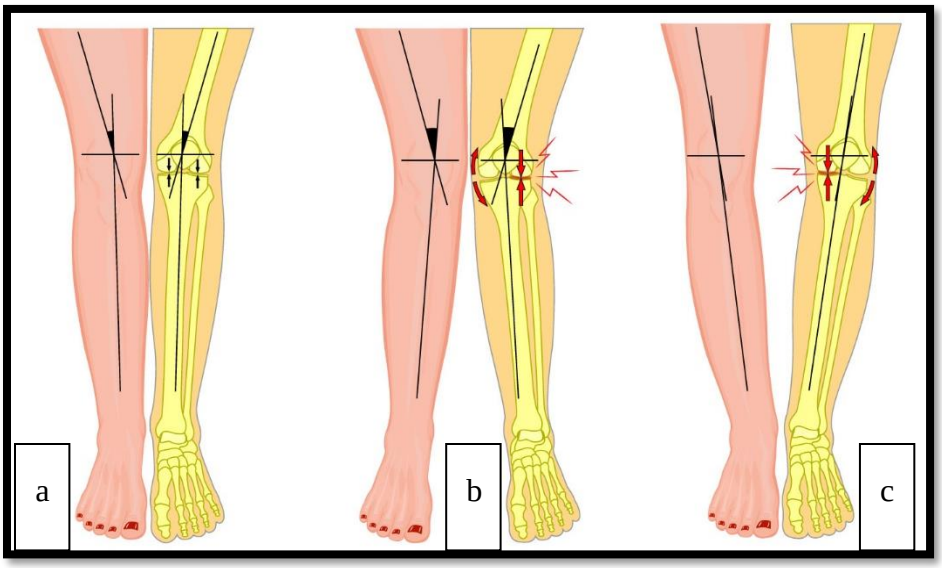

Figure 2.7 Force distribution in a) normal knee, b) Valgus knee, and c) Varus knee (Fitness, 2019).

To restore the mechanical alignment of the knee, the proximal tibia is resected perpendicular to the tibial shaft, and the distal femur is cut in 6-degree valgus to the femoral anatomical axis (Fig. 2.8) (John N. Insall, 1993).

Another method for bone resection is the axial plane alignment of the femoral implant based on the landmarks.

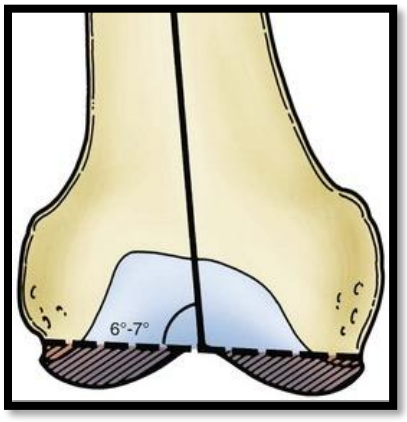

Figure 2.8 Final outcome of the distal femur (Thomas Parker Vail, 2016).

Fig. 2.9 illustrates three bone landmarks, namely: The posterior condylar axis, The epicondylar axis, and Whiteside's line (Babazadeh et al., 2009). Alignment with this method needs the universal cutting box.

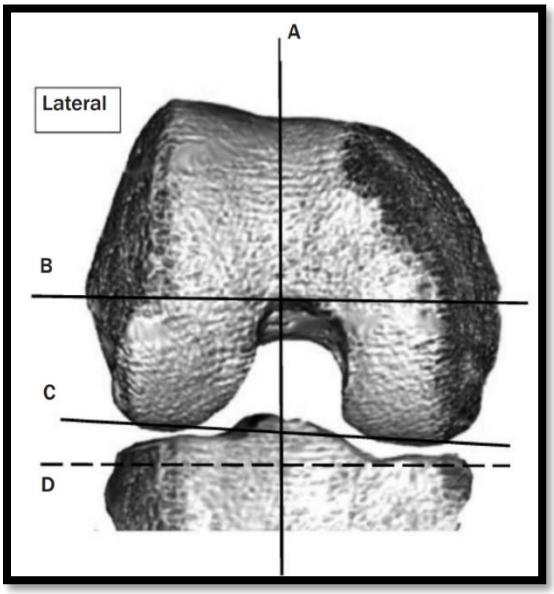

Figure 2.9 (A) the anteroposterior trochlear sulcus (Whiteside's line), (B) epicondylar axis, (C) posterior condylar axis, and (D) tibial bony cut (Babazadeh et al., 2009).

2.8.2 Instrumentation for TKA

There are several techniques for surgeons to achieve the required component position and restoration of the mechanical alignment in TKA. The cutting blocks used to do the resections were first positioned by using mechanical jigs that were modified to match the patient's landmarks. After the surgeon places the cutting blocks, the accuracy of this technique is dependent on the surgeon's ability to properly identify landmarks. To enhance the bone preparation, navigation TKA which show the patient's limb alignment in real time, was developed. Finally, the most recent advancement in TKA is the patient specific TKA which eliminates registration time of optical navigation systems.

2.8.2.1 Mechanical Jigs

The goal of restoring mechanical alignment is obtained by performing appropriate cuts at the femoral and tibial distal. To identify the main landmarks of the bone, extramedullary and

intramedullary alignment (IM) guides are used. It has been more common among the surgeons to use intramedullary shafts for femoral alignment, while tibial extramedullary rods are more popular for tibial cut. In the intramedullary alignment system, the intramedullary canal should be drilled for the shaft to be inserted into the bone, which might cause the bone fracture. Extramedullary alignment in the tibia is used to reduce the risk of bone fracture and precision loss in valgus tibia (John N. Insall, 1993).

In the intramedullary femoral alignment system, the distal femoral cutting guide and cutting box are attach to the alignment shaft. The IM alignment guide inserts into the intramedullary canal (Fig. 2.10), and the proper angle of the distal cut is determined based on the position of intramedullary canal and mechanical axis. After placing the intramedullary rod, the distal cut guide is attached. In bone resection method with extramedullary tibial rod, the rod is clamped distally around the malleoli until the spike of the tibial reference is fully inserted into the tibia. Then, the proximal tibia cut guide and saw slot can be attached to rod in the desirable level (Solution, 1995).

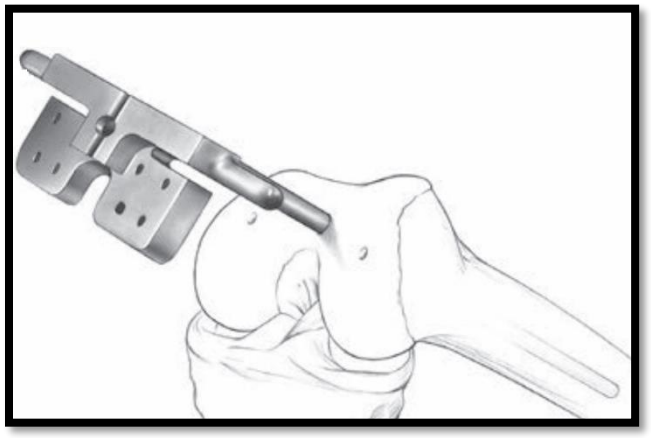

Figure 2.10 Insertion of the IM alignment guide into the femur (Solution, 1995).

2.8.2.2 Computer-assisted surgery in Total Knee Replacement (CAS – TKA)

The CAS navigation has been established to reach the intraoperative alignment by navigating anatomical data and transferring alignment feedbacks to the surgeon. The rate of CAS navigation has grown from 2.4 percent in 2003 to 33.2 percent in 2018, according to the Australian

Orthopaedic Association National Joint Replacement Registry (AOANJRR) (*National Joint Replacement Registry AOA Hip*, 2021).

In general, there are three different modalities for CAS systems: image-based, image-free modalities, and handheld accelerometer-based navigation systems (recently improved). In image-based type, a 3D model of the knee is created from preoperative Magnetic resonance imaging (MRI) and computerized tomography (CT) (Jones & Jerabek, 2018; Frederic Picard et al., 2016). Implant alignment with image-free surgical navigation systems, track optically the bone positions of femur, tibia, and surgical instruments. An optical navigation system a 3D camera is installed and fixed on a cart that contains the navigation computer.

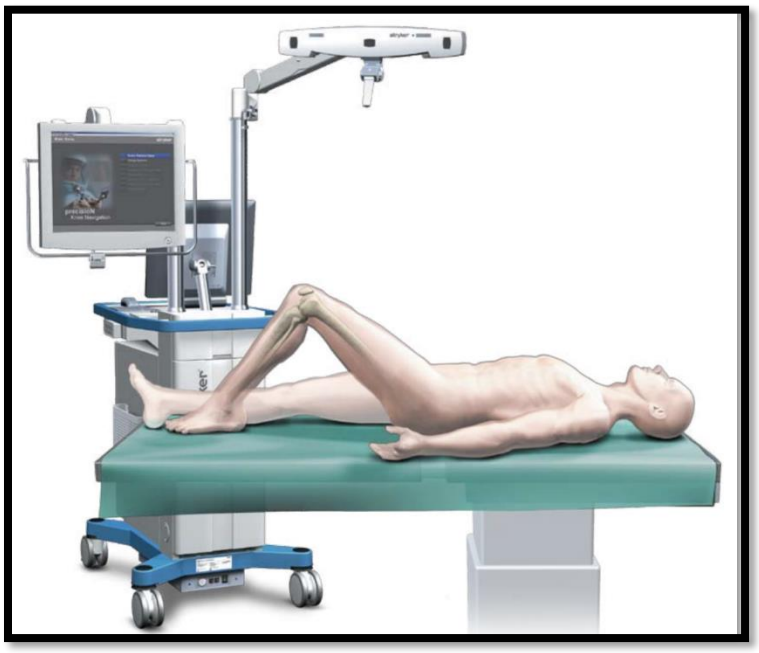

Figure 2.11 The Stryker Navigation System using interactive operative monitoring system (Stryker, 2007b).

The markers contain infrared LEDs which are detected by 3D camera during the time system is activated. These markers are mounted on the femoral and tibial anchoring devices, and they could be tracked during surgery (Stryker, 2007b).

Figure 2.12 The Stryker Femur/Tibia tracker (Stryker, 2007a).

Mostly all navigation systems have virtual bone models to establish the surgical plan. To generate the personalized surgical plan, virtual bone models should be matched to the patient's landmarks in the registration step. There are mainly four registration process models, Fiducial based, Landmark-based registration, Intensity-based registration, and bone-shaped based (Sugano, 2003). Fiducial-based registration contains more surgical steps to place fiducial screws into the femur and tibia while the CT scan is made. The risk of local inflammation, infection, and pain are reasons for complications of the fiducial method (Stiehl et al., 2007; Sugano, 2003).

Shape-based registration which is also called "bone morphing" collects information of patient's bone surface to create a 3D model of the real bone, which could be matched to the preoperative 3D image. For bone registration, single points or point clouds are taken over landmarks to create the surgical plan. An additional process called bone morphing might also be used in the point clouds to create the patient bone model. After all information from patient's anatomy is conveyed to the navigation system, the system evaluates varus/valgus angle, flexion/extension angle, and resection volume (Stiehl et al., 2007).

Infrared light is utilized in an imageless CAS navigation system for tracking the various patient anatomy landmarks around the knee. The virtual coordinate system generated by imageless CAS provides surgeons with calculations to evaluate bone cuts on the femur and tibial and lets them check the performed cuts (Frédéric Picard et al., 2007; Siston et al., 2007).

While most of the CAS systems are using optical navigation systems, other alternatives like handheld and surface-mounted CAS navigation have been introduced to TKA surgery recently (Figueroa et al., 2018). One of these handheld systems that relies on accelerometer-based navigation is iASSIST (Denis Nam et al., 2013).

2.8.2.3 Robotic Navigation

Robotic-assisted surgery is a type of surgery in which a surgeon's skill is combined with computer-navigation and robotically cutting guides. Robotic navigation systems are wildly used for presurgical planning and intraoperative haptic feedback, with arm-assisted and robotic-guided cutting jigs methods (David J Allen Jacofsky, 2016). Schneider and Troccaz (Schneider & Troccaz, 2001) had classified four types of the robots based on their technology design to passive, active, interactive, and tele-operated. Passive systems contain a robotic arm or device, which needs interaction from surgeon to completely control the surgery procedure. While active robots are autonomous and employ preoperative and intraoperative planning data to cut the bone, without any participation of the surgeon (Schneider & Troccaz, 2001).

Some models of Robotic navigations that are commercially available are listed bellow:

2.8.2.3.1 MAKO

The Mako Robotic-Arm Interactive System is marketed by Stryker Orthopaedics (Mahwah, NJ, USA) (Fig 2.13). MAKO technology creates a personalized implant that matches to patient’s knee anatomy. This robot is defined as a semi-active robot with a haptic interface (Pailhé et al., 2021). This guides the surgeon to perform the bone cuts in the preoperatively planned boundaries, therefore it improves knee alignment restoration and ligament balancing ("Pros & Cons of Robotic-Assisted Surgery," 2014).

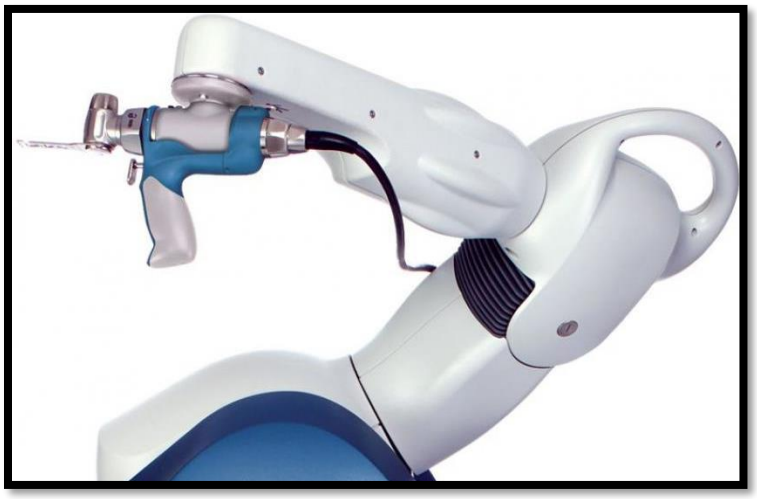

Figure 2.13 Mako®, ©Stryker Orthopaedics ("Stryker celebrates 1,000th install of Mako System," 2020).

2.8.2.3.2 NAVIO

NAVIO is a semi-active surgical system that allows the surgeon to characterize the bone and cartilage in real-time. The bone resection and gap balancing are performed by reamer which contains an end-cutting burr in the navigation field to remove the bone in the preoperative plan. However, no requirement to the preoperative CT scan is one of the main advantages of this system, reaching a flat bone cut using a reamer is not easy (David J. Allen Jacofsky, 2016).

Figure 2.14 Navio®, ©Smith & Nephew ("Smith & Nephew Launches NAVIO for Total Knee," 2017).

2.8.2.3.3 ROSA

Another robot with the interactive robotic platform is the ROSA Knee robot, created by Zimmer-Biomet (Warsaw, IN, USA). Base on the navigation data provided by optical trackers attached to the patient's leg, ROSA creates a 3D model of the knee in real-time. The surgeon uses this intraoperative plan for positioning the cutting guides, which are attached to the robotic arm, on the knee (Pailhé et al., 2021).

Figure 2.15 Rosa Knee®, ©Zimmer-Biomet ("ROSA Knee System," 2022).

2.8.2.4 The accelerometer-based navigation system

Higher alignment precision and less blood loss are the most evident benefits of adopting a computer navigation system in TKA compared to traditional procedures (Browne et al., 2010). However, the steep learning curve, difficulties with pin sites such as infection and pain, the longer mean operating time, drawbacks of dealing with sensitive optical sensors, and greater capital costs are negative aspects that limited the large use of CAS techniques (Jones & Jerabek, 2018). Hand-held navigation systems based on accelerometers appear to be a potential alternative to large console CAS systems in TKA to address the benefits of CAS while reducing its shortcomings. The first generation of accelerometer-based navigation systems contains a small display console attached to an EM tibial or IM femoral jig, which displays alignment information in real-time. The tibial/femoral jigs are used to establish the mechanical axis and the cutting block is pinned to the bone for performing the resection (Denis Nam et al., 2012). Figure 2.16

shows The KneeAlign2 TM system (OrthAlign Inc., Aliso Viejo, CA), which is an accelerometer-based navigation system for performing bone resection on the proximal tibial and distal femoral in TKA (Denis Nam et al., 2012).

Figure 2.16 Image of the KneeAlign2 TM system for performing the proximal tibial (Denis Nam et al., 2013).

2.9 iASSIST

2.9.1 navigation systems

The iASSIST (Zimmer, Inc., Warsaw, IN, USA) knee system is a portable navigation device, using inertial electronic components for the tracking process. Combining the alignment precision of large-console CAS systems with the simplicity of conventional alignment methods, grabbed many surgeons' attention to this easy-to-use technology. The navigation system of iASSIST is designed based on using disposable electronic pods which are attached to the femoral and tibial resection instruments. These pods contain inertial electronic components of accelerometer and gyroscopes that communicate wirelessly with each other (Kinney et al., 2018).

iASSIST is an extramedullary alignment (EM) cutting guide that is affixed to the bone using the same pins used for the conventional method, without any intrusive into the intramedullary canal of tibia. In addition, the resection instruments of tibial and femoral jigs, and surgical workflow of iASSIST is highly like the conventional method. These similarity to the conventional method makes more familiarity for the surgeon and led to a shorter learning curve. During the surgery procedure, the surgeon can check the alignment data on the tablet or the user interface of the pods which are attached to the resection guide devices and cut the bone at the proper angle in both sagittal and coronal planes. The surgeon can also validate the accuracy of the alignment after bone resection is done and any adjustment can be applied at this point (Goh et al., 2016). This intelligent cutting block system offers intraoperative verification for both stages of surgery, bone cuts and overall alignment, which improves postoperative functional outcomes. After the bone resection, the surgeon can validate the accuracy of the alignment and apply any adjustment needed. The iASSIST knee system provides a wide variety of adjustments in Varus/Valgus and Flexion/Extension. The surgeon can adjust the Tibia slope in the range of 0 to 9º, while this amount is ±3º for varus/valgus.

Comparing the iASSIST navigation system with conventional TKA shows that the occurrence of malalignment is significantly lower in the iASSIST group. This number is 13.3% for iASSIST group, compared with 29.04% in the conventional group (Li et al., 2019). On the other hand, comparing the iASSIST with CAS system shows that many shortcomings of CAS have been reduced in the iASSIST system. In the accelerometer-based electronic components systems like iASSIST, the preoperative imaging step of CAS is not needed, and the complicated registration process with a large computer console is not required (Li et al., 2019).

The surgical workflow follows the classic method of femoral and tibia bone resection with each bone resected independently along the mechanical axis. The following section describes the surgical technique for the iAssist system.

2.9.2 Surgical technique for the iAssist system:

The surgical technique for the iASSIST system has been explained in this section based on the prototype images. The tip of the spike of the Upper Tibial Reference of the extramedullary guide

impacts at the mechanical axis entry point between the tibial spines (Fig. 2.17). The instrument shaft is oriented to align with the medial third of the tubercle.

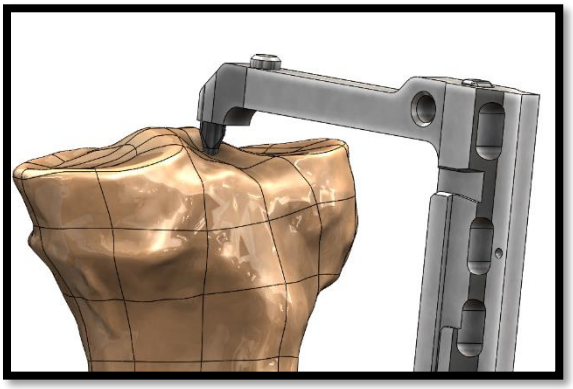

Figure 2.17 The cylinder part of the spike in the entry point of the mechanical axis.

The distal clamps around the malleoli are firmly gripped and, the spike is impacted until the fins are fully inserted in the tibia. These self-centering clamps over the malleoli ensure that the instrumentation was fixed over the center of the ankle and remain securely positioned on the malleoli (Fig. 2.18. a). Figure 2.18. b. shows the assembly of Tibial Proximal Cut Guide, A/P Slider, and Adjustment Mechanism are inserted onto the Upper Tibial Reference.

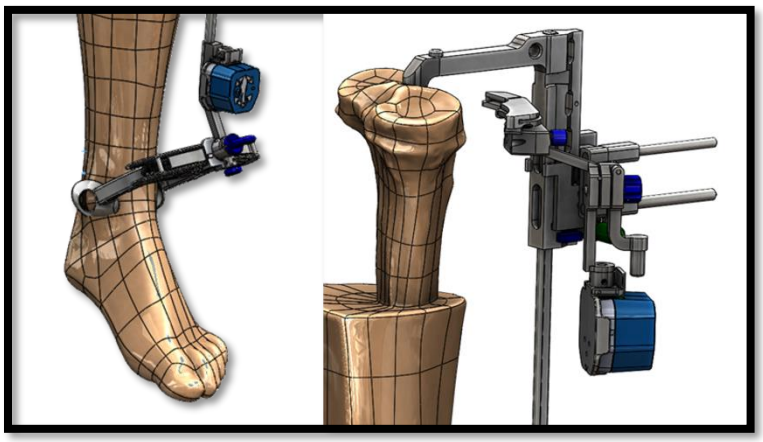

Figure 2.18 a) The cylinder part of the spike in the entry point of the mechanical axis, and b) The Upper Tibial Reference is assembled on the Lower Tibial Reference and the reference pod is clipped to it.

After the Upper Tibial Reference is positioned between the tibial spines in the center of the tibial joint surface, the distal portion of the Lower Tibial Reference is positioned on the malleoli. The

next step is proceeding with the Tibia V2 Cut Guidance. The Z button of either the Cut Guide Pod or the Reference Pod helps to start Tibia V2 Cut Guidance. Red and green LEDs on the Cut Guide Pod attached to the Proximal Cut Guide give feedback and adjust the tibia slope and varus/valgus using the gold and green screws, respectively. Fig. 2.19. Shows the Saw slot assembly along with the Upper Tibial Reference Secure and the Distal Cut Guide onto the tibia by inserting three pins (two in the upper parallel holes and one in the lower diagonal medial hole).

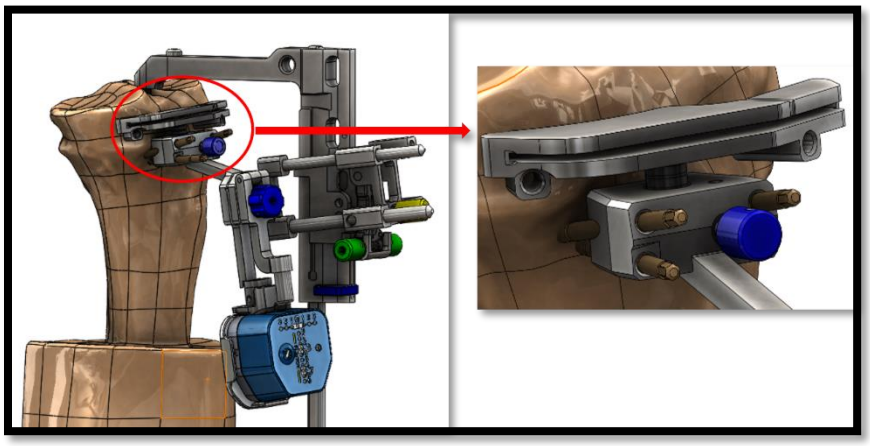

Figure 2.19 Surgeon inserts three pins in the Cut Guide Pin holes (one in each of the 2 parallel holes on the top and one in the medial hole at the bottom)

With the leg flexed at more than 45° and the knee stable, the Tibial A/P slider is unlocked by using the blue screw to initiate the coordinates transfer. The knee should be held steady until the coordinate transfer confirmation sound is heard. This allows for the information of the Reference Pod (being removed) to transfer to the Cut Guide Pod (staying on the bone). A confirmation sound is heard when the disconnection and the information transfer have been completed between the two pods.

The surgeon removes the Lower Tibial Reference from the leg leaving only the Cut Guide (with the Saw Slot) pinned on the bone. The Reference Pod from the Lower Tibial Reference is removed and assembles on the Validation Tool. The Validation Tool on which the Reference Pod is assembled, helps the surgeon performs the validation of the cut (Fig. 2.20). The validation makes it possible to display the angles in Flexion/Extension and Varus/Valgus of the cut that has been made.

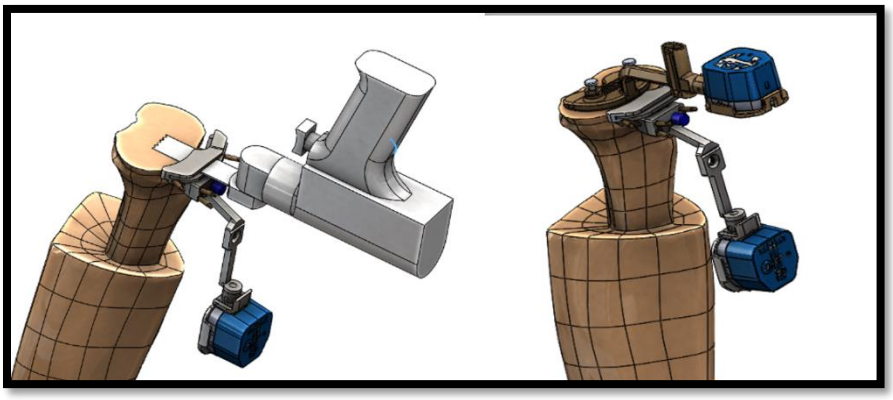

Figure 2.20 a) Performing the resection. b) Surgeon performs the validation of the cut with the Validation Tool on which the Reference Pod is assembled.

2.10 Pins Interference in the iAssist Knee Instruments for Tibia V2

Figure 2.21. illustrates prototype design of the Upper Tibial Reference instrument used in the iAssist Knee Instruments for Tibia V2. As it has been shown in Fig. 21, the prototype of the Upper Tibial Reference contains a long and a short spike which are inserted into the patient's bone to fix the instrument during the procedure.

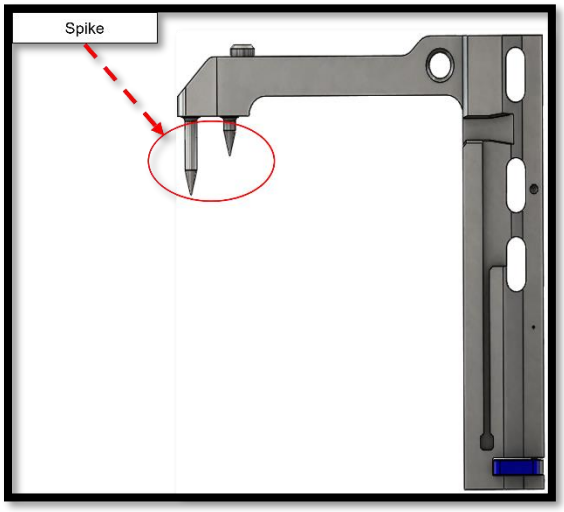

Figure 2.21 Solid works drawing of prototype sample of Upper Tibial Reference used in the iAssist Knee Instruments for Tibia V2.

On the other hand, a five 3.2mm Headless Trocar Drill Pin is inserted into the bone to fix the Tibial Proximal Cut Guide on the tibia (See Fig. 2.22). As it can be seen in Fig. 2.22, a risk of interference has been identified between the 3.2mm Headless Trocar Drill Pins and the Long Spike that is 20mm-long.

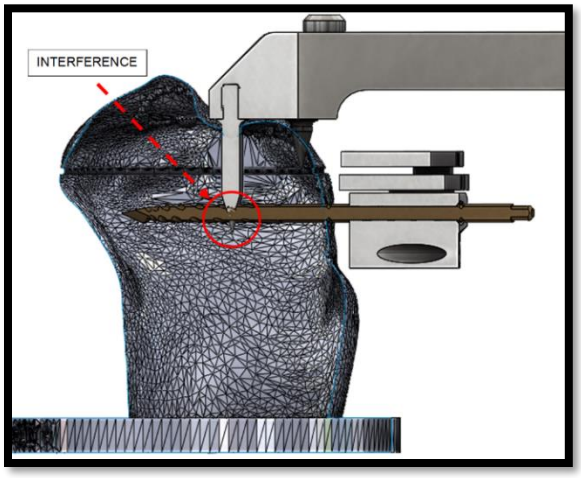

Figure 2.22 Illustration of the interference between the pins and the long spike.

2.11 Introduction to Tibial Reference instrument for Tibia V2

The risk of pin interference between the long spike of the Upper Tibial Reference of Tibia V2 and the pins to be inserted in the Cut Guide, lead to redesign the original TR with two spikes. As it has been shown in Fig. 2.23, The new design for TR contains a single spike having fins to better anchor the Tibial Reference and acting as the second spike of the original design to block the rotation of the instrument around the mechanical axis.

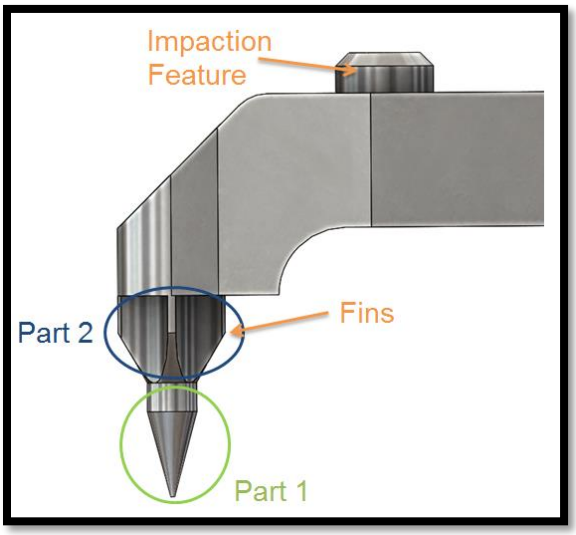

Figure 2.23 New design for the Upper Tibial Reference instrument with description of the different parts of the spike.

2.12 Design Controls (21 CFR Part 820.30)

From concept to market launch, developing a new medical device is a complex process. One of the primary procedures outlined in 21 CFR Part 820.30 is design controls which is a regulatory requirement for medical devices. These design control regulations must apply to the design and development of any new products to ensure that specified design requirements are met ("code of Federal regulation," 2022). This process includes identifying and documenting user needs, as well as design input and output, performing design reviews, verification, and validation, and appropriately executing design transfer and changes.

According to Iso 13485 chapter 7.3.3 (“Design and development inputs”), function, performance, and safety requirements should be used as the basis for designing purposes. These requirements for developing a new device should be determined, evaluated, and documented. Design output is the result of each design phase and at the end of the total design effort, it is a basis for the device master record.

For medical device companies, a complete record of the design and development of a device should be recorded. The FDA requires in 21 CFR Part 820.30 a Design History File DHF, in

which all the documentation that shows the evolution of the design, should be assembled. One of the most important aspects of DHF is design verification and validation activities that verifies if the design meets the system requirements and specifications. Fig. 2.24. Represent a visual relationship between design verification and validation.

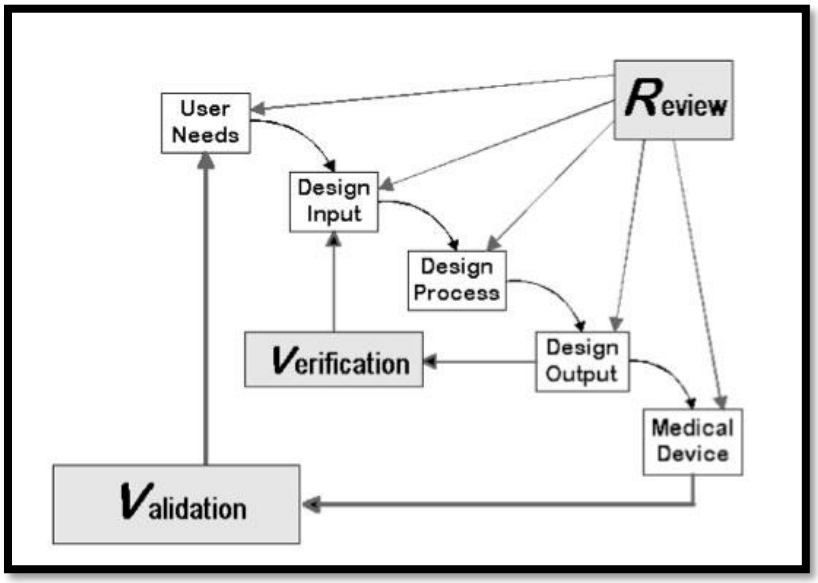

Figure 2.24 FDA CDRH 1997 Design Control Guidance for Medical Device Manufacturers.

CHAPTER 3 THESIS OBJECTIVES

The aim of this study is to characterize the stability of the most recent Tibial Reference instrument designed at Zimmer Biomet for Total knee surgery. This new tibial instrumentation is designed for the iAssist Knee system V3, which use an extramedullary guide to make the tibial plateau cut. The cutting guide includes a malleoli clamp which is fixed around the ankle and a cutting block for proximal tibial cut. A connecting shaft is fixed on the bone with Tibial Reference instrument. The surgeon can cut the tibial plateau precisely with predetermined angle relatively to the mechanical axis to the mechanical axis using this iASSIST knee alignment.

The new designed Upper Tibial Reference contains a new instrument and new surgical technique with a spike that will be inserted into the tibia. For the system to be accurate, the Tibial Reference needs to be stable in the bone. Therefore, the stability of this instrument is a factor that should be characterized when impacted into the bone. The main objective of this test is to characterize the error caused by the instability of the insertion of the Tibial Reference spike into the bone. In this project, the Faro Arm, a portable coordinate measuring machine (CMM), helps to calculate all the measurements related to the rotation (in terms of rotation, varus/valgus, and tibial slope in relation with the tibia mechanical axis) and translation between the bone and the Tibial Reference at multiple key points during the surgical flow. The instability error is obtained from the difference of rotation and translation between the key points.

To validate the test method used for determining the instability error, a test method validation (TMV) should be implemented. We will explore in our second objective, the repeatability and reproducibility of the following critical test parameters:

- CMM measurements of the inserts used for positioning references on osteroporotic bone
- CMM measurements of the Upper Tibial Reference

So, the goal of the TMV study is to prove the repeatability and reproducibility of the measurements with the Faro CMM arm.

The third objective is to verify that the transformation matrix method provides accurate angle results.

The primary outcome measures are improving the accuracy and precision of total knee arthroplasty during component positioning and therefore overall limb alignment.

The hope is that this information will give us a better understanding of how the new design for Tibial Reference is stable on the tibia bone. This would allow for optimum TKA stability for patients which will allow for possible improved patient satisfaction and implant survival.

Once the instruments were created, their performance and instabilities were then verified experimentally with the manufactured components and tibia sawbones model.

CHAPTER 4 THE TEST METHOD FOR TIBIAL REFERENCE SPIKE INSTABILITY CHARACTERIZATION

4.1 Objective:

As it has been mentioned in chapter 2, for the iAssist Knee system V3 at Zimmer Biomet, a new tibial instrumentation is designed. This new instrumentation contains a new instrument and new surgical technique with a spike that will be inserted into the tibia. For the system to be accurate, the Tibial Reference needs to be stable in the bone. Therefore, the stability of this instrument is a factor that should be characterized when impacted into the bone. The main objective of this test is to characterize the error caused by the instability of the insertion of the Tibial Reference spike into the bone.

4.2 Materials and Method:

The main materials needed for this test are the Upper Tibial Reference instrument, the Faro CMM arm and osteoporotic sawbones. Following the surgical flow protocol, the Tibial Reference is installed on the sawbones. The CMM arm help to calculate all the measurements defined in this study. The CMM arm is used to measure the rotation (in terms of rotation, varus/valgus and tibial slope in relation with the tibia mechanical axis) and translation between the bone and the Tibial Reference at multiple key points during the surgical flow. The instability error is obtained from the difference of rotation and translation between the key points.

4.2.1 Sample size:

Since this test is a characterization test and does not have an acceptance criteria, it is not possible to define a confidence and reliability level. However, according to Process Validation

Acceptance Activities at Zimmer, the minimum number of samples to determine normality is 20. The sample size for this test will thus be 20.

4.2.2 Set up description:

Seven sawbones are labeled from one to seven, and three holes were drilled into the cortex at positions of R1, R2 and R3 (See Fig. 4.1). Before inserting the CMM prob in the holes, some epoxy was placed in the holes. Each insert into the hole is referred as reference divots.

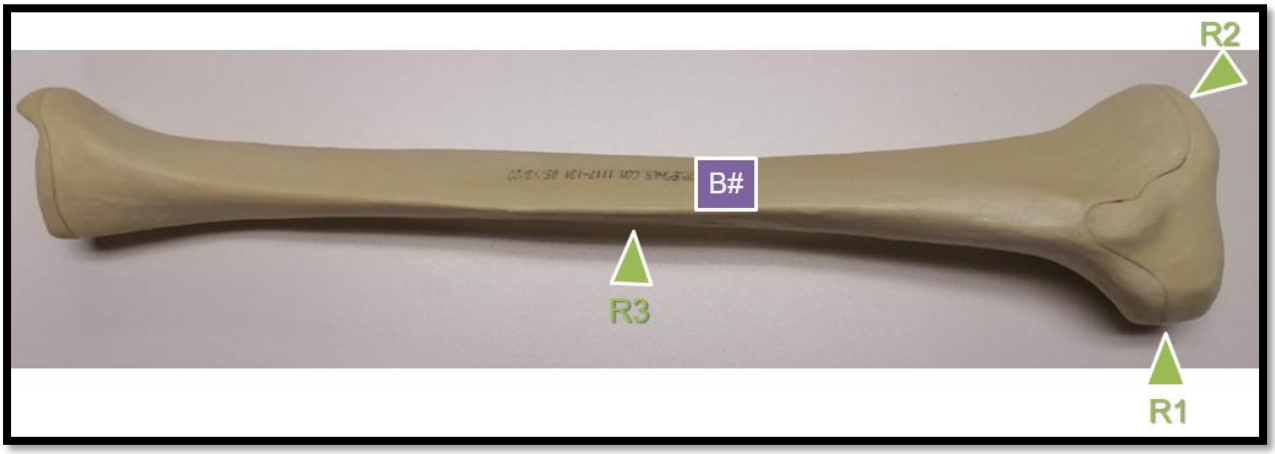

Figure 4.1 Placement of the divots on the sawbone.

Figure. 4.2. Illustrates the process of installing the malleoli simulator onto the sawbones. Tibial clamps were used to install the sawbones on the articulated bone holder (See Fig. 4.2), and some cable ties were used to fix the sawbones on the holder to reduce any possible movement during probing with CMM.

Figure 4.2 The sawbone and FARO arm are installed on the table.

The Tibial Reference was installed on the sawbone as defined in the surgical technique. The Tibial Reference spike was impacted into the approximate S1, S2, and S3 location, as it has been shown in Fig. 4.3. For each sample a measurement file was created on the Faro software.

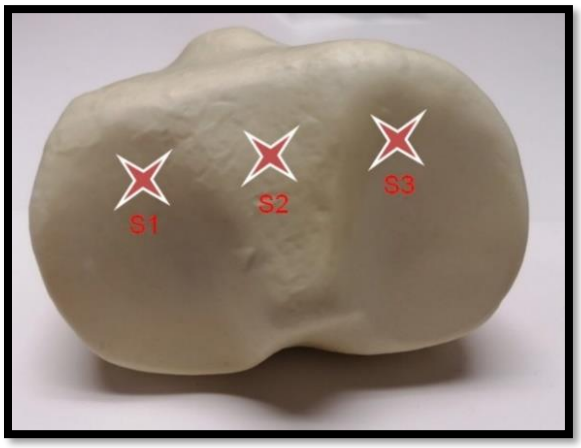

Figure 4.3 Approximate location of the Tibial Reference Spike Impaction.

4.2.3 Measurement instructions:

The probe was placed on three different planes, plane P1, plane P2 and plane P3 of the Upper Tibial Reference (Fig. 4.4). For each plane, 10 points distributed along the plan's surface. On the bone side, probe was inserted into the R1, R2 and R3 divots, as it was illustrated in Fig. 4.1. For each sample 5 points at different probe angulations were taken for the first set of measurements.

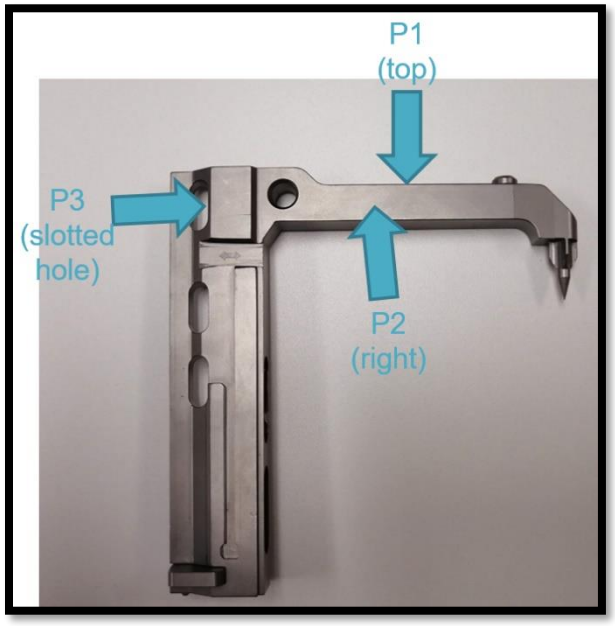

Figure 4.4 Measurements to take on the Upper Tibial Reference.

In purpose of calculating the instability error related to insertion of Upper Tibial Reference to the bone, a partial flow of surgery was implemented. The Adjustment Mechanism assembly (Adjustment Mechanism, Cut Guide and A/P slider) was installed on the Tibial Reference as per surgical technique. Then, the assembly was removed, and it was installed again. The Reference pod was clipped onto the Lower Tibial Reference and the Cut Guide pod was clipped to the Cut Guide instrument. The Z button of the Cut Guide was pressed, and the second measure was taken following measurement instructions for the Tibial Reference and the bone.

The flexion extension of the cut plane was adjusted. The articulated bone holder was unlocked the leg was brought about 30 degrees more in extension. The leg was brought back at its initial position and the articulated bone holder was locked. The Saw Slot was inserted into the Cut Guide. The Slope was adjusted and Varus/Valgus on the Adjustment Mechanism to 7 degrees slope and 0 degrees V/V. The cut guide was pushed against the bone. The height of the cut was adjusted with the stylus. The cut guide to the bone was pinned with 3 pins following the surgical technique. The third measure was taken following measurement instructions for the Tibial Reference and the bone.

In last step, the AP slider was disconnected, and the Saw slot height was adjusted by pushing on the button. The fourth measure following measurement instructions described following measurement instructions for the Tibial Reference and the bone.

The final output of the test comes from the calculation of the transformation matrix, which comes from the CAM2 software. Calculations are applied to the transformation matrix to get angles in Varus/Valgus, Flexion/Extension (Tibial Slope) and Rotation (See Fig. 4.5).

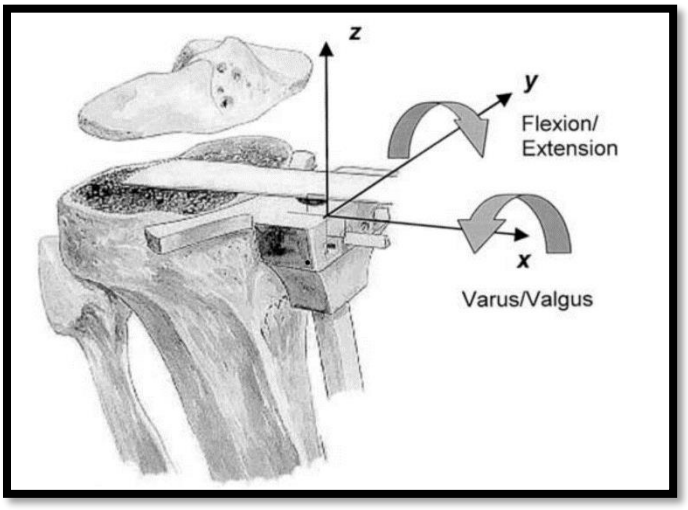

Figure 4.5 The bone-cutting errors in the sagittal plane are Flexion-extension errors (y), and varus-valgus errors are in the frontal plane (x) (Plaskos et al., 2002).

4.2.4 Statistical Analysis

4.2.5 Explanation for calculation of instability

The instability error is calculated by subtracting the position of the Tibial Reference after the A/P slider disconnection to the position of the Tibial Reference after the Z button is pressed. This allows to consider displacements of the instrument during the entirety of tibia v2 navigation flow.

$$Instability\ Error\ = Measure\ 4\ - Measure\ 2$$

There are 4 rotation matrixes for each of the 20 samples, and 3 Euler angles (XYZ) and translation are defined for each of those rotation matrixes. The stability error is calculated from subtraction of one set of Euler angles. From the 4-rotation matrix, three stability errors are calculated, and each has the following parameters: Δrotation, ΔVarus/Valgus, Δslope, Δtranslation.

Calculations will be necessary to transform the exported euler angles into the desired angles (rotation, V/V and tibial slope). The resection angles are defined the following way (see figure 4.5 for visual representation):

The rotation angle is the angle between the projection of the x vector of the sawbone coordinate system on the XY plane, defined by the coordinate system of the tibial reference. That corresponds to take the arctangent of the first and second value of the first column of the rotation matrix.

The varus/valgus angle is the angle between the projection of the z vector of the sawbone coordinate system on the YZ plane, defined by the coordinate system of the tibial reference. That corresponds to take the arctangent of the second and third value of the third column of the rotation matrix.

The flexion/extension angle is the angle between the projection of the z vector of the sawbone coordinate system on the ZX plane, defined by the coordinate system of the tibial reference. That corresponds to take the arctangent of the first and third value of the third column of the rotation matrix.

The relative orientations in varus/valgus, flexion/extension (tibial slope) and rotation are thus calculated at each step of the flow and the variation is obtained by subtracting the angular values between each step.

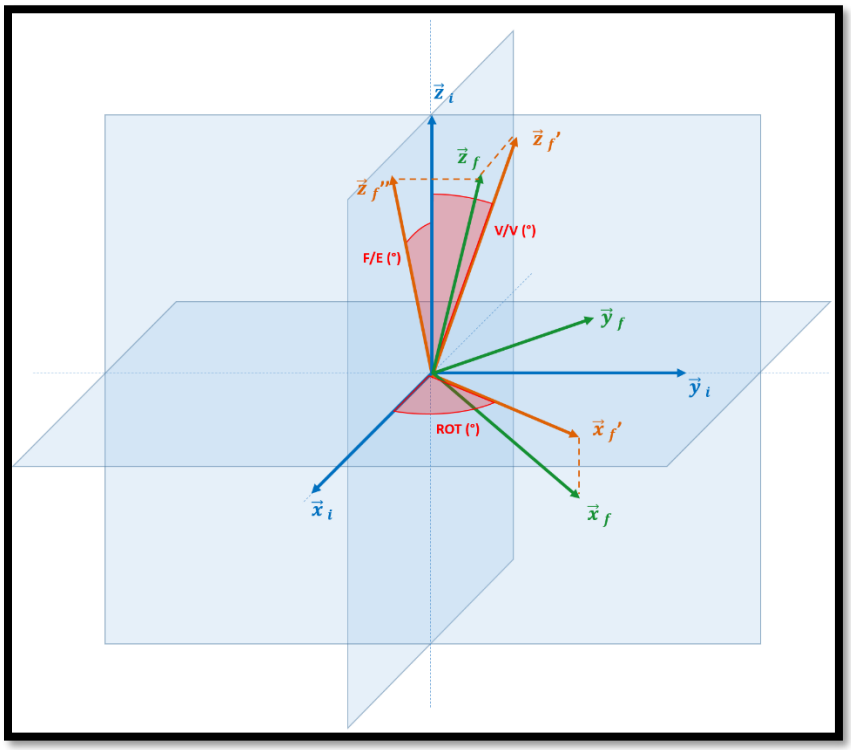

Figure 4.6 Explanation of projection angles calculation.

All the data from the euler files were copied and pasted in one Excel file. On Minitab, for each 15 groups from the Excell file, the option Display Descriptive Statistics was selected from the Excel file. The following statistics: Mean, SE of mean, Standard deviation, Minimum, Variance, Maximum and Median were calculated. If the P-value was superior to 0.05, the distribution was considered normal. For the groups with normal distribution, 3 sigma and 6 sigma were calculated. To determine which step of the surgical flow causes the most movement, an ANOVA

analysis between the 3 Rotation groups was performed, the 3 V/V groups, the 3 Slope groups and the 3 translation groups.

4.3 Results:

As it has been explained in method section, measurements were performed at 4 different surgery stages:

1. Installation of Tibial Reference instrument.
2. Installation of other instruments, pods and pressing the Z button.
3. Adjustment of F/E and V/V and pinning of the cut guide to the bone.
4. Disconnection of the A/P slider.

It was determined that the 1st measurement is not useful for the characterization of the instability error, as the system only acquires the mechanical axis of the tibia when the Z button is pressed (measure 2). Therefore, the displacement of the instrument between measure 1 and 2 does not have an impact on the accuracy of the system and will thus not be considered for the iAssist knee system stack-up.

4.3.1 The instability error of the Tibial Reference instrument on osteoporotic bone

The area under the probability curve in which 67 percent of all errors occur is defined by one standard deviation on either side of the mean. 95 percent of all errors are contained within two standard deviations and 99 percent of all errors are related to three standard deviations. In this section the normality test of all three parameters of Rotation, Flexion/Extension, and

Varus/Valgus are investigated in purpose of calculating the descriptive statistics. Instability Error of the Tibial Reference instrument is calculated with $|\mu| + 3\sigma$ equation.

4.3.1.1 Rotation

Figure 4.6. shows that the Anderson-Darling normality test was passed (p-value ≥ 0,05) for the rotation instability data. The distribution is thus normal.

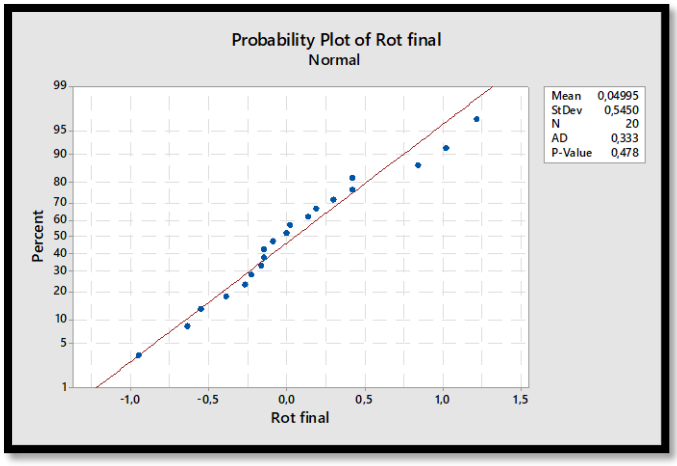

Figure 4.7 Result of the Anderson-Darling normality test for Rotation parameter

The descriptive statistics for Rotation parameters are shown in Table 4.1.

Table 4.1 descriptive statistics for Rotation parameter

Mean (μ)	Standard deviation (σ)	Minimum	Q1	Median	Q3	Maximum
0.05	0.545	-0.948	-0.258	-0.044	0.389	1.218

4.3.1.2 Varus/Valgus

An Anderson-Darling normality test was executed and passed (p-value ≥ 0.05) with the Varus/Valgus instability data. The distribution is thus normal (See Fig. 4.7).

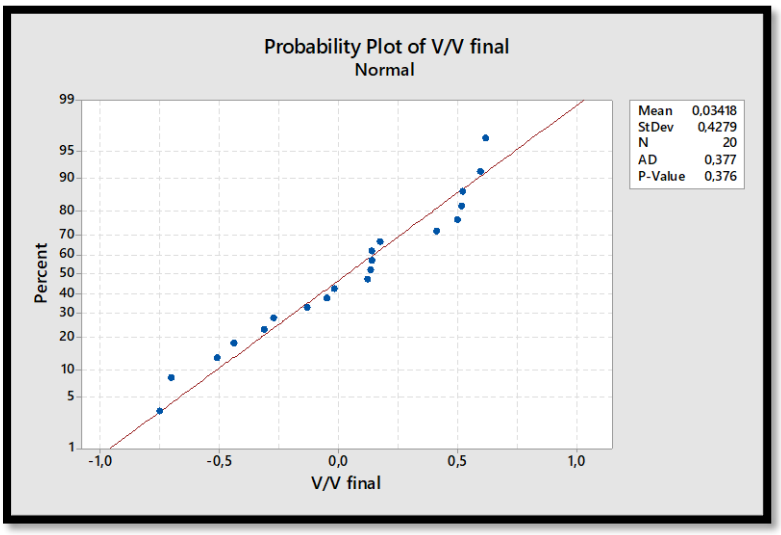

Figure 4.8 Result of the Anderson-Darling normality test for Varus/Valgus parameter.

The descriptive statistics for Rotation parameters are shown in Table 4.2.

Table 4.2 descriptive statistics for Varus/Valgus parameter.

Mean (μ)	Standard deviation (σ)	Minimum	Q1	Median	Q3	Maximum
0.034	0.428	-0.753	-0.302	0.129	0.479	0.617

4.3.1.3 Flexion/Extension

The flexion/extension parameter was failed in all three different normality tests with p-value ≤ 0,05.

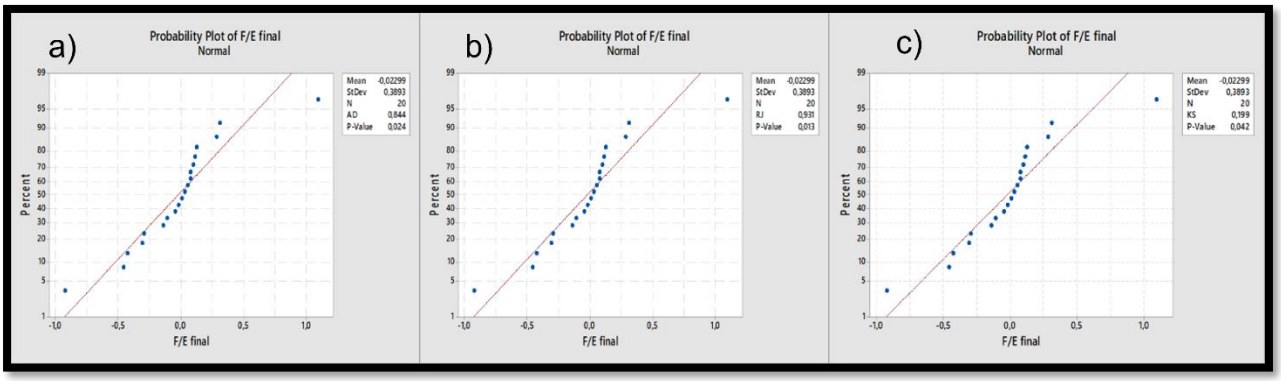

Figure 4.9 Normality tests with F/E parameter a) Anderson-Darling b) Ryan-Joiner c) Kolmogorov-Smirnov.

As it has been shown in Figure 4.8, the distribution is not normal. The Johnson transformation was used to transform the distribution into a normal one (Fig. 4.9).

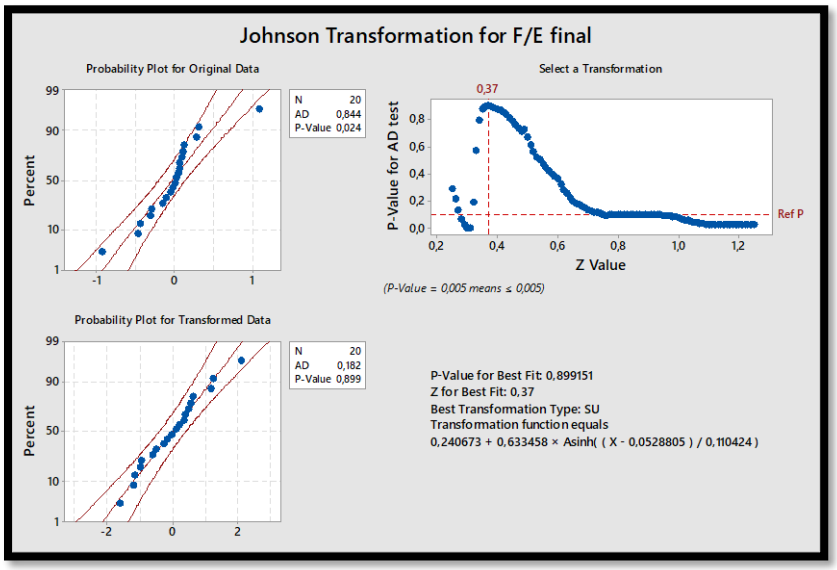

Figure 4.10 Jonhson transformation of the Flexion/Extension parameter.

Table 4.3 descriptive statistics for Flexion/Extension parameter.

Mean (μ)	Standard deviation (σ)	Minimum	Q1	Median	Q3	Maximum
0.010	0.198	-0.925	-0.256	0.019	0.108	1.094

4.3.2 Summary of instability error results

Table 4.4 summarizes the instability error results for all 3 parameters.

Table 4.4 Rotation, V/V and F/E instability error results.

Parameter	Instability Error ($\|\mu\| + 3\sigma$)	Instability Error (mm)
Rotation	1.6885°	0.29
Varus/Valgus	1.3179°	0.23
Flexion/Extension	0.6035°	0.1

To convert this angle into millimeters, the following calculation was applied. The varus valgus plane on the Tibial Reference is the lateral plane used to measure the coordinate system and its lenghth is 10 mm.

Stability error $_{mm}$ = (length of the V/V plane on the TR) × Tan (stability error $_{degrees}$)

4.3.3 Impact of location of impaction of Tibial Reference

Each sawbone was used 3 or 4 different times on a different location on the bone. This helped to increase the number of tests that could be executed per sawbone. To determine how different location impact on the results, an ANOVA test was used. As it has been shown in Table 4.5, all the p-values were over 0.05, for Rotation, Varus/Valgus and Flexion/Extension. It can be

concluded that the location of the impaction of the Tibial Reference did not have an impact on the results of this test. Since all the p-values were all well over 0.05, it can be concluded that the location of the impaction of the Tibial Reference did not have an impact on the results of this test.

Table 4.5 P-Value for Rotation, V/V and F/E parameters.

Parameter	$p-value$
Rotation	0.908
Varus/Valgus	0.975
Flexion/Extension	0.555

4.3.4 The highest source of instability

Means of instability for different steps of the flow for Rotation, V/V, and F/E parameters are reported in table 4.6. By comparing three instability results of 1-2, 2-3, and 3-4 steps, we can identify which phase caused the most movement of the Tibial Reference in the bone.

An ANOVA was used to confirm that the three groups had significantly different means (p-value ≤ 0.05) for the Rotation and Flexion/Extension parameters. The null hypothesis of ANOVA states that all means are equal, thus we can reject it and infer that not all means are equal in this test.

Table 4.6 Table Means of instability for different steps of the flow for Rotation, V/V, and F/E.

Parameter	Comparison	Mean
Rot	1-2	0.1597°
	2-3	0.5103°
	3-4	0.2079°
V/V	1-2	0.2356°
	2-3	0.2975°
	3-4	0.1258°
F/E	1-2	0.2393°
	2-3	0.5045°
	3-4	0.3908°

Results from Table 4.6 and one-way ANOVA analysis demonstrate that the movements executed between measures 2 and 3 (insertion of the saw slot, adjustments of F/E and V/V, pinning the cut guide to the bone) have the highest impact on instability error for the Rotation and Flexion/extension parameters.

4.4 Discussion

In general, free play of instruments in bone should be minimal in all mechanisms of iASSIST knee system to avoid adding angular error to the navigation system. In the present study, to evaluate the stability of the newly designed Tibial Reference for the iASSIST knee system, a part of surgery flow was implemented on the sawbones model. In similar stages of surgery, Tibial References were inserted into the bone model during 4 steps. In each step, the displacement of the instrument in the bone is the factor that was measured with the FARO CMM arm. It should be mentioned, this study is a characterization test that has been implemented to the iASSIST knee instrument for the first time. So far, to our knowledge, there are not any other similar published studies to compare the results. However, learning the methods used in calculating the instability of miniscrew in the orthopedic might be inspiring to some extent (Oga et al., 2019). For the groups with normal distribution, 3 sigmas were calculated. Calculation of 3 sigmas has been introduced as instability error in this study to characterize data to be able to make a judgment about how the process is performing in the future. Instability error results for Rotation, V/V, and F/E parameters are reported in table 4.4 in degree and millimeters. These errors could affect the acquisition of landmarks and the calculated gap values.

In this study, each sawbone was used in three different spots for the insertion of the Tibial Reference spike. Thus, results could be impacted by the factor of location of TR insertion. However, the ANOVA test (table 4.5) shows that the results of this test are not affected by the location of the impaction of the Tibial Reference. It is important to note that there is thus no potential for an altered relationship in the real surgery, as the spike of TR inserts in only one place of real bone. Furthermore, the difference between mechanical properties of sawbones with real bones might result in different displacement of Tibial Reference spike into the sawbones compare to real bone. Hence, the iASSIST knee system should perform more accurately compared to this study.

Another important outcome of this study was indicating the highest source of instability. Comparing means of instability for different steps of the surgery flows (table 4.6) revealed that the movements executed between measures 2 and 3 have the highest impact on instability error for the Rotation and Flexion/extension parameters. This stage relates to the insertion of the saw slot, adjustments of F/E and V/V, pinning the cut guide to the bone.

To verify the total accuracy and precision of the system, the overall error should be recognized. This error could affect the acquisition of landmarks and the calculated gap values. The stability of the mechanical axis due to the fixation of the rocket spike feature into the bone is part of the overall error which has been addressed in this study.

CHAPTER 5 TEST METHOD VALIDATION FOR TIBIAL REFERENCE SPIKE INSTABILITY CHARACTERIZATION

This test method validation will validate the test method described in chapter 4 for the verification of Tibial Reference Spike Instability Characterization.

The first objective of this test is to assess the repeatability and reproducibility of the following critical test parameters:

- CMM measurements of the inserts used for positioning references on osteroporotic bone
- CMM measurements of the Upper Tibial Reference

The second objective is to verify that the transformation matrix method described in chapter 4, provides accurate angle results.

The third objective is to justify bounds of the critical parameters are not expected to influence test results.

In this chapter, variation between each operator will be examined. The Residual Sum of Squares (RSS) of the Tibial Reference and bone variations (in Varus/Valgus, Flexion/Extension and Rotation) will be considered as the measurement error and will be used in system stack-up.

5.1 Method:

The Tibial Reference instrument, the Faro CMM arm, and osteoporotic sawbones will be used for this test. Three operators are used to take 3 measurements of 8 bones and 7 Tibia References. As it has been mentioned in chapter 4, the probe was placed on three different planes, plane P1, plane P2 and plane P3 of the Tibial Reference (Fig. 4.4). On the bone side, probe was inserted into the R1, R2 and R3 divots, as it was illustrated in Fig. 4.1. This test is separated in three phases. In phases 1 and 2 the dimensional inspection of the Upper Tibial Reference instrument

and the osteoporotic bone are reported. Transformation matrixes will be exported from the measured coordinates system and their variability analyzed.

Phase 3 will be used to verify the accuracy of the transformation matrix and calculations method used to determine angles in Varus/Valgus, Flexion/Extension (Tibia Slope) and Rotation.

5.2 Statistical analysis:

Statistical analysis and calculations are presented in this section. Dimensional inspection of the inserts used for positioning the references (bone models). Three parameters of Rot, V/V and F/E are investigated individually. Three normality tests, Anderson-Darling, Ryan-Joiner and Kolmogorov-Smirnov with a confidence of 95% are used to analyze the normality of each distribution. Each test must pass one or more of these normality tests to be considered as a normal distribution. In case a distribution was not normal, transformations were used to obtain descriptive statistics to characterize the measurement error of the test, which is one objective of this TMV. The parameters were also submitted to an ANOVA study to determine if results were influenced by the user or the sample. The Minitab software was used for the statistical analysis.

The goal of executing an ANOVA statistical analysis is to identify the variances of two different variables are significantly different, and in this study those two variables are users and samples. If data sets are not significantly different, this proves the repeatability and reproducibility of the measurements with the Faro arm, which is the main objective of this Test Method Validation study.

5.3 Results:

5.3.1 Phase 1: Dimensional Inspection of the inserts used for positioning the references (bone models)

5.3.1.1 Rotation:

As it has been shown in Fig. 5.1, the rotation parameter passed the normal distribution test of residuals (the p-value is higher than 0.05).

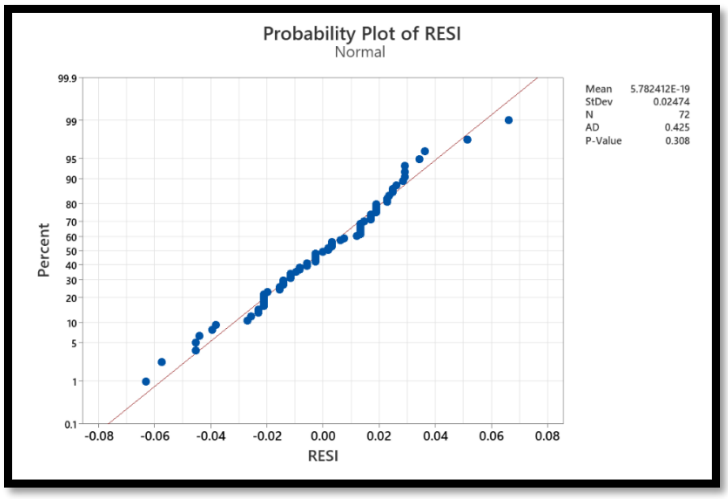

Figure 5.1 Normal probability plot of the residuals for Rotation parameter of bone models.

Results of ANOVA for Rotation parameter from bone model is described in table 5.1. The p-values higher than 0.05 show the Rotation parameter does not vary in function of the User or Sample, and these two parameters are independent.

Table 5.1 Results of ANOVA for Rotation for bone model

Parameter	Number of groups	P-value
User	3	0.137
Sample	8	1.000

Descriptive statistics were obtained with Minitab are presented in table 5.2.

Table 5.2 Descriptive statistic for the Rotation parameter of bone models.

Mean (μ)	Standard Deviation (σ)	99,7% value (μ + 3 σ)
-0.002	0.027	0.008

5.3.1.2 Varus/Valgus:

The Varus/Valgus parameter failed the normal distribution test of residuals (the p-value is inferior to 0.05), as described in Figure 5.2.

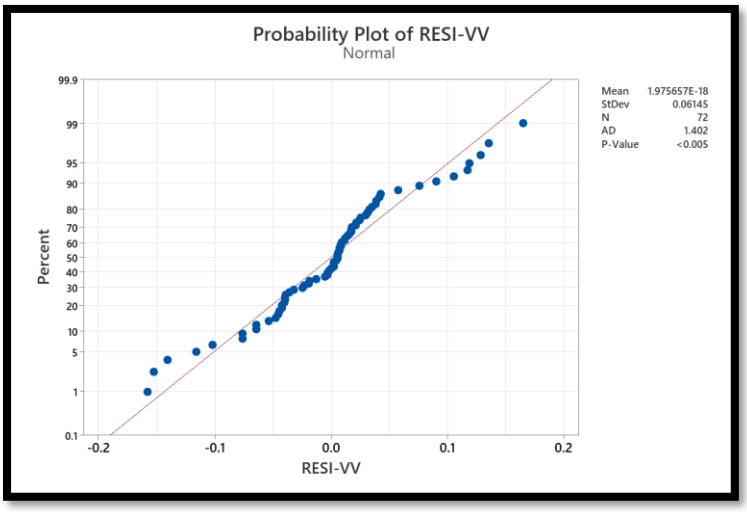

Figure 5.2 Normal probability plot of the residuals for Varus/Valgus parameter for bone models.

Transformations had to be applied to get a normal distribution for the V/V parameter. In this situation, the box cox transformation cannot be used because there are negative values. The Johnson transformation was used instead.

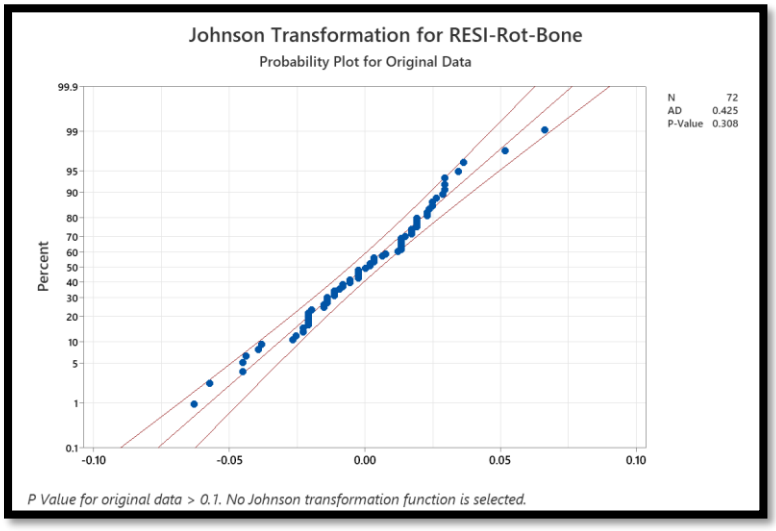

Figure 5.3 Jonhson transformation of the residuals for Varus/Valgus parameter of bone model.

An ANOVA was performed on the transformed values, and results are presented in Table. 5.3.

Table 5.3 Results of ANOVA for Varus/Valgus for bone model

Parameter	Number of groups	P-value
User	3	0.025
Sample	8	0.008

As it has been shown in Table 5.3, the p-value for the Sample and User parameters is under 0.05. This value shows that the Sample and User parameters are not independent and do influence the results. This would define that the results of the test will vary in function of the user and the bone model.

Descriptive statistics were obtained with Minitab and presented in table 5.4.

Table 5.4 Descriptive statistic for the V/V parameter of bone models

Mean (μ)	Standard Deviation (σ)	99,7% value (μ + 3σ)
0.007	0.051	0.160

5.3.1.3 Flexion/Extension:

The Flexion/Extension parameter failed the normal distribution test of residuals (the p-value is inferior to 0.05), as described in Figure 5.5.

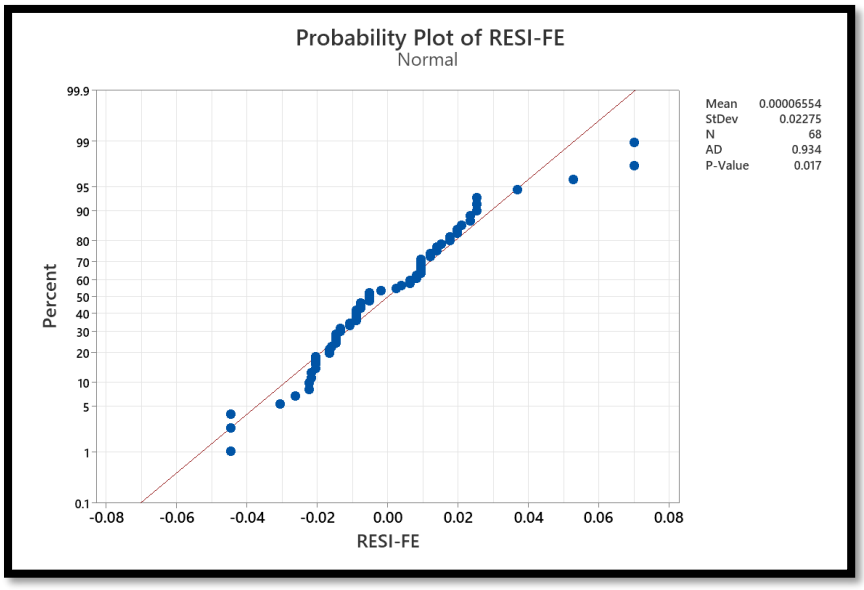

Figure 5.4 Normal probability plot of the residuals for Flexion/Extension parameter for bone models.

Transformations had to be applied to get a normal distribution for the Flexion/Extension parameter. In this situation, the box cox transformation cannot be used because there are negative values. The Jonhson transformation was used instead as described in figure 5.6.

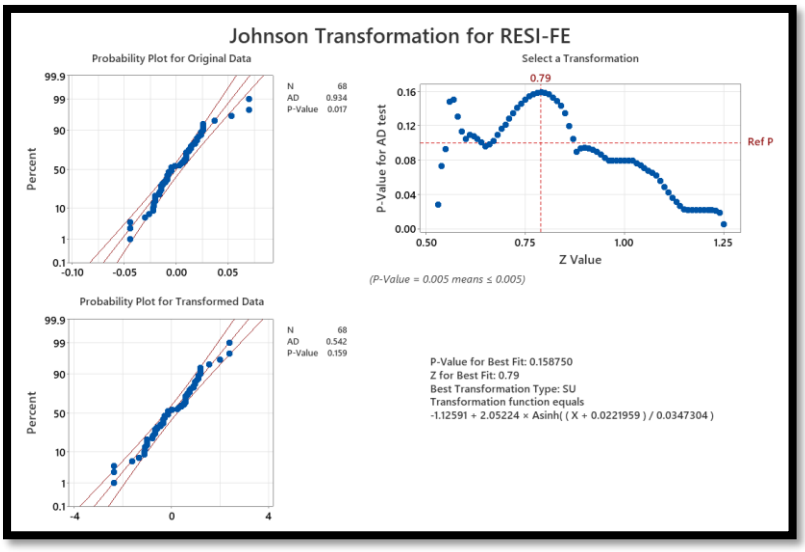

Figure 5.5 Jonhson transformation for Flextion/Extension parameter of bone model.

Descriptive statistics were obtained with Minitab on the transformed values with the Johnson equation, as presented in table 5.8.

Table 5.5 Descriptive statistic for the F/E parameter of bone models

Mean (μ)	Standard Deviation (σ)	99,7% value (μ + 3 σ)
0.014	1.024	0.413

Finally, an ANOVA was performed on the transformed values (Table. 5.6).

Table 5.6 Results of ANOVA for Flexion/Extension for bone model.

Parameter	Number of groups	P-value
User	3	0.716
Sample	8	0.019

The P-values obtained from ANOVA test for User and Sample parameters are 0.716 and 0.019 respectively, which is inferior to the 0.05 value for the samples (See table. 5.6). This made the rejection of the null hypothesis. This would define that the results of the test will vary in function of the samples the bone model.

5.3.2 Phase 2: Dimensional Inspection of the Upper Tibial Reference

For dimensional inspection of the Upper Tibial Reference, each parameter of Rotation, Flexion/Extension and Valgus/Versus was investigated individually. The normality of each distribution was tested, and transformations were used in case a distribution was not normal. The parameters were also submitted to an ANOVA study to determine if results were influenced by the user or the sample. The Minitab software was used for the statistical analysis.

5.3.2.1 Rotation

As it has been shown in Fig. 5.7, the rotation parameter of Tibial Reference instrument failed the normal distribution test of residuals (the p-value is higher than 0.05).

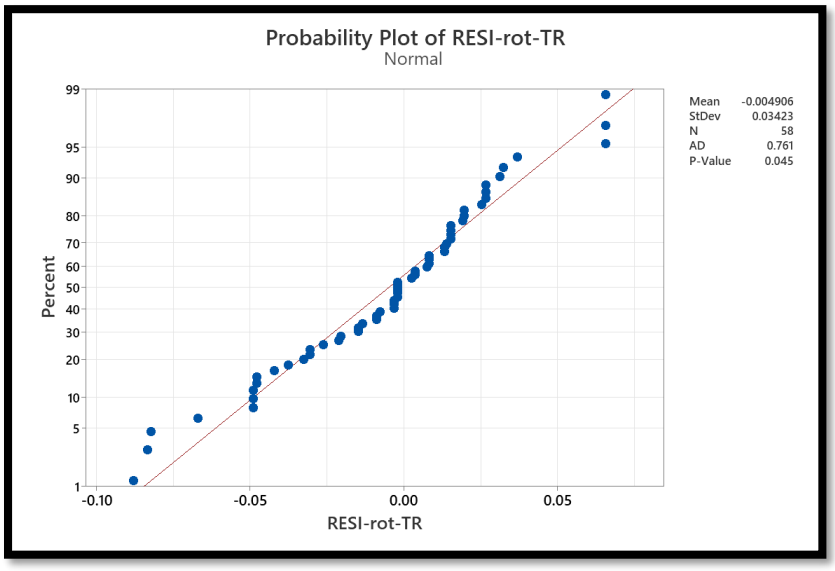

Figure 5.6 Normality tests for Rotation parameter for Tibial Reference

Transformations were applied to get a normal distribution for the Rot parameter. In this situation, the box cox transformation cannot be used because there are negative values, so the Jonhson transformation was used instead as described in Figure 5.8.

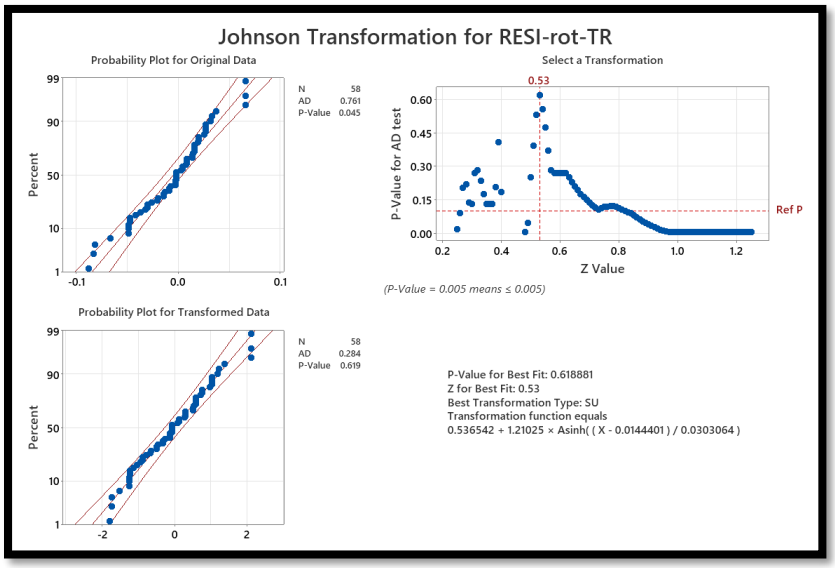

Figure 5.7 Johnson transformation for rotation parameter of Tibial Reference.

Finally, an ANOVA was performed on the transformed values:

Table 5.7 Results of ANOVA for Rotation for TR.

Parameter	Number of groups	P-value
User	3	0.268
Sample	7	0.079

The p-values being ≥ 0.05 mean that the Rotation parameter does not vary in function of the User or Sample.

Descriptive statistics were obtained with Minitab on the transformed values with the Jonhson equation, as presented in table 5.8.

Table 5.8 Descriptive statistic for the Rotation parameter of Tibial Reference instrument

Mean (μ)	Standard Deviation (α)	99.7% value (μ + 3α)
-0.031	0.964	0.366

5.3.2.2 Varus/Valgus

The Varus/Valgus parameter passed the normal distribution test of residuals (the p-value is higher than 0.05), as described in Figure 5.9.

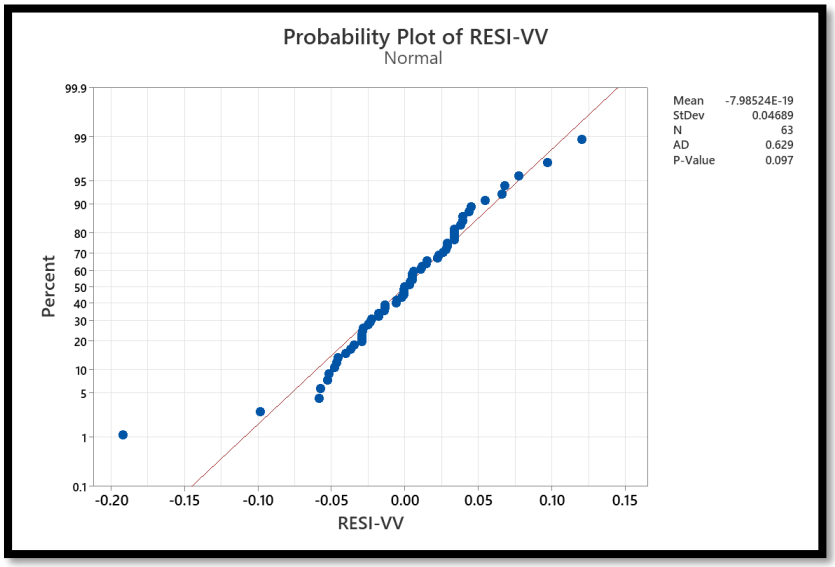

Figure 5.8 Normal probability plot of the residuals for Varus/Valgus parameter for Tibial Reference instrument.

The ANOVA results are presented in table 5.11:

Table 5.9 Results of ANOVA for Varus/Valgus for TR

Parameter	Number of groups	P-value
User	3	1.00
Sample	7	0.588

The p-values being ≥ 0.05 mean that the Varus/Valgus parameter does not vary in function of the User or Sample.

Descriptive statistics were obtained with Minitab and presented in table 5.10.

Table 5.10 Descriptive statistic for the Varus/Valgus parameter of Tibial Reference instrument.

Mean (μ)	Standard Deviation (σ)	99,7% value (μ + 3 σ)
-0.00001	0.047	0.020

5.3.2.3 Flexion/Extension

The Flexion/Extension passed normality tests for the residuals (the p-value is higher than 0.05), as described in Figure 5.10.

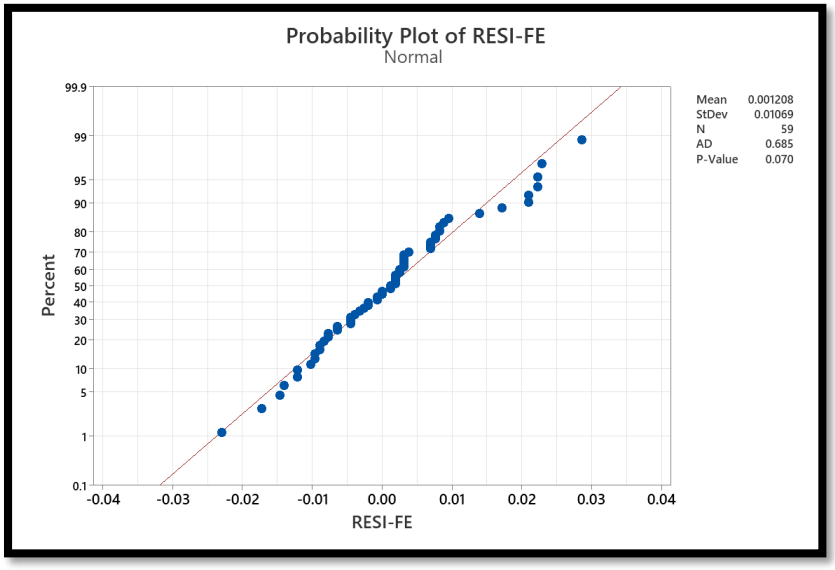

Figure 5.9 Normality tests for Flexion/Extension parameter for Tibial Reference.

Table 5.11 Results of ANOVA for Flexion/Extension for TR

Parameter	Number of groups	P-value
User	3	0.641
Sample	7	0.088

For the ANOVA test, the p-values being ≥ 0,05 mean that the Flexion/Extension parameter does not vary in function of the User or Sample. Descriptive statistic was obtained as presented in table 5.11.

Table 5.12 Descriptive statistic for the Flexion/Extension parameter of Tibial Reference instrument.

Mean (μ)	Standard Deviation (α)	99,7% value (μ + 3α)
-0.00001	0.047	0.020

5.3.3 Phase 3. Verification of the Transformation matrix method accuracy

To verify if the transformation matrix method provides an accuracy measure of angles, a gage block with known angles is used (Fig. 5.11).

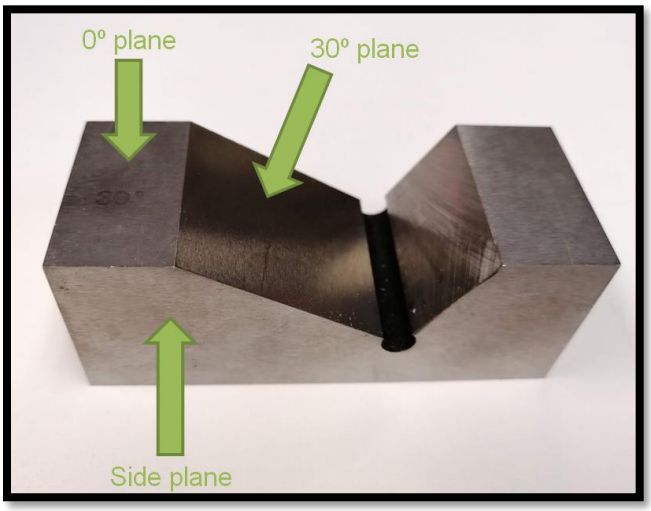

Figure 5.10 Acquisition planes of the gage block.

Phase 3 was executed by User 1 and only require a sample of 1. The following results were obtained (table 5.13):

Table 5.13 The angles calculated from projection of coordinate matrix on the gage block.

Rot	Projection of X3 in the XY plane
	-3.330
V/V	Projection of Z3 in the YZ plane
	-29.840
F/E	Projection of Z3 in the ZX plane
	1.057

The angle of -29,844 degrees that was obtained for the V/V angle can be rounded up to the theoretical 30 degrees of the gage block. This means that the transformation matrix method is accurate.

5.3.4 Combination of Phase 1 and Phase 2

The objective of this test was to measure the error from the test method. To do this, the error (99,7% value (μ + 3α)) from the bone models and the Tibial Reference instruments had to be combined. The Root Sum of Squares (RSS) method was used, and all the results are in degree.

Rotation:

$$Error_{Rotation} = \sqrt{Error\ rot\ bone^2 + Error\ rot\ Tibial\ Reference^2} = \sqrt{0.028^2 + 0.964^2} = 0.964$$

Varus/Valgus:

$$Error_{Rotation} = \sqrt{Error\ v/v\ bone^2 + Error\ v/v\ Tibial\ Reference^2} = \sqrt{0.050737^2 + 0.04689^2} = 0.69$$

Flexion/Extension:

$$Error_{Rotation} = \sqrt{Error\ f/e\ bone^2 + Error\ f/e\ Tibial\ Reference^2} = \sqrt{0.047^2 + 1.024^2} = 1.025$$

5.4 Discussion

The first goal of this test is to assess the repeatability and reproducibility of The Faro CMM measurements. CMM measurements of the inserts for positioning references on osteoporotic bone and CMM measurements of the Upper Tibial Reference were investigated in this test. The final output of the test came from the calculation of the transformation matrix, produced by the

CAM2 software. Calculations are applied to the transformation matrix to get angles in Varus/Valgus, Flexion/Extension, and Rotation.

Dimensional inspection of the inserts used for positioning references is a critical test, as it is related to the error of the measuring technique. Determination of this error is necessary to assess the validity of measurements which will become an input of the system stack-up.

For each sample of bone models or Tibial Reference instrument, two-ways ANOVAs were performed on each parameter of rotation, varus/valgus, and flexion/extension. The null hypothesis for the ANOVA test is that there is no difference between means. To show neither the sample nor the user had significant impact on the measure, the p-value of each parameter was measured. This amount of p-value is superior to 0.05, except for V/V and F/E parameters of bone models which means that the null hypothesis is rejected. As this test method was not able to detect the cause of variation in the system and rejection of the null hypothesis for ANOVA test, a Gage R&R study is conducted to this project in purpose of investigating the variation of the measurement system.

Another investigation that was applied in this section is verifying if the transformation matrix method described in chapter 4 provides accurate angle results. One of the interests for this phase is to determine the V/V angle. The amount of -29.844 degrees angle was rounded up to the theoretical 30 degrees of the gage block. This means that the transformation matrix method is accurate.

CHAPTER 6 GAGE R&R ANALYSIS

As per QI03-M1 Rev.16 Mechanical Design at Zimmer, Production Equivalent Units (PEU) have to meet some requirements in order to be usable for the Validation & Verification activities of the project. Among these requirements, all the CTQs (Critical to Quality dimensions) have to have a successful Gage R&R study. In the following chapter a study of Gage R&R is conducted to determine the total variation of the measurment system.

The gage repeatability and reproducibility (Gage R&R) analysis states that whether the measurement system is suitable for its intended purpose or not. The aim of this study is also to indicate which part of the measuring system causes the most deviations of measurement. Therefore, the ANOVA-based GR&R studies is used for this study to detect any possible operator-part interaction. Although an in-depth discussion of GR&R is beyond the objectives of this study, a quick overview of the application is provided below.

According to Minitab 20 support definition:

- Repeatability is stated as “how much variability in the measurement system is caused by the measurement device”. In other words, this is an index that demonstrates a measurement system's capacity to produce consistent results from repeated measurements. (Kazerouni et al., 2009)

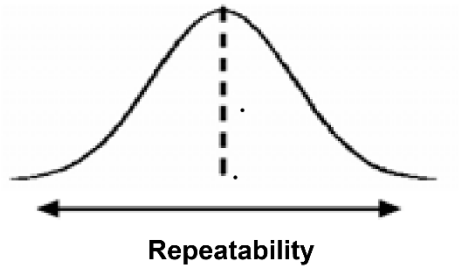

Figure 6.1. Repeatability (Kazerouni et al., 2009)

- Reproducibility is “how much variability in the measurement system is caused by differences between operators”. In fact, Reproducibility refers to the variation of human factors when employing the same equipment and procedure (Kazerouni et al., 2009).

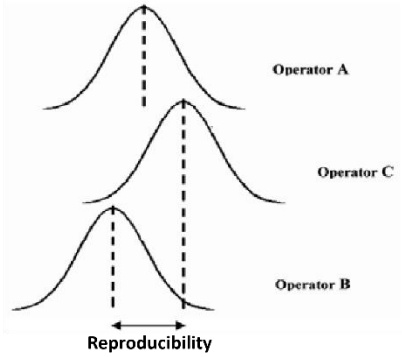

Figure 6.2. Reproducibility (Kazerouni et al., 2009)

- Total Gage R&R is "The sum of the repeatability and the reproducibility variance components".
- Part-to-Part variation is "The variability in measurements due to different parts".

According to AIAG (2002) the acceptance criteria is: (AIAG. (2002). Measurement Systems Analysis, Reference Manual, Third Edition. Southfield, Michigan: Automotive Industry Action Group.)

- if the % Gage R&R is under 10%, the measurement system is acceptable.
- if the % Gage R&R is between 10% and 30%, a measurement system may be acceptable for some application.
- If the % Gage R&R is over 30%, the measurement system is considered unacceptable.

6.1 Method:

This study was conducted to Gage R&R to evaluate the Repeatability and Reproducibility of the measurement system for bone samples. In this test, three operators measured the same sample three times using the same gauge, under the same conditions. Gage repeatability and reproducibility calculates total variation to determine how much variation is attributable to

appraisers and equipment (%R&R). Each appraiser followed the same procedure and steps, to obtain the data.

The numerical data were entered into the MINITAB20 data analysis program. MINITAB is a comprehensive statistical and graphical analysis software package that analyzes the data to produce relevant results.

6.2 Results:

6.2.1 Gage study for Bone model:

The data results for each parameter of Rot, V/V and F/E parameters of bone models are visualized in Figures 6.3, 6.4 and 6.5. To help clarify the results, key numbers from the original data have been used. Based on the findings of this investigation, it was determined that the present measurement system is insufficient to conduct the necessary measuring tasks.

The following Gage R&R data result for CMM machine on the Rot parameter of bone model is used as a sample to explain some key result numbers.

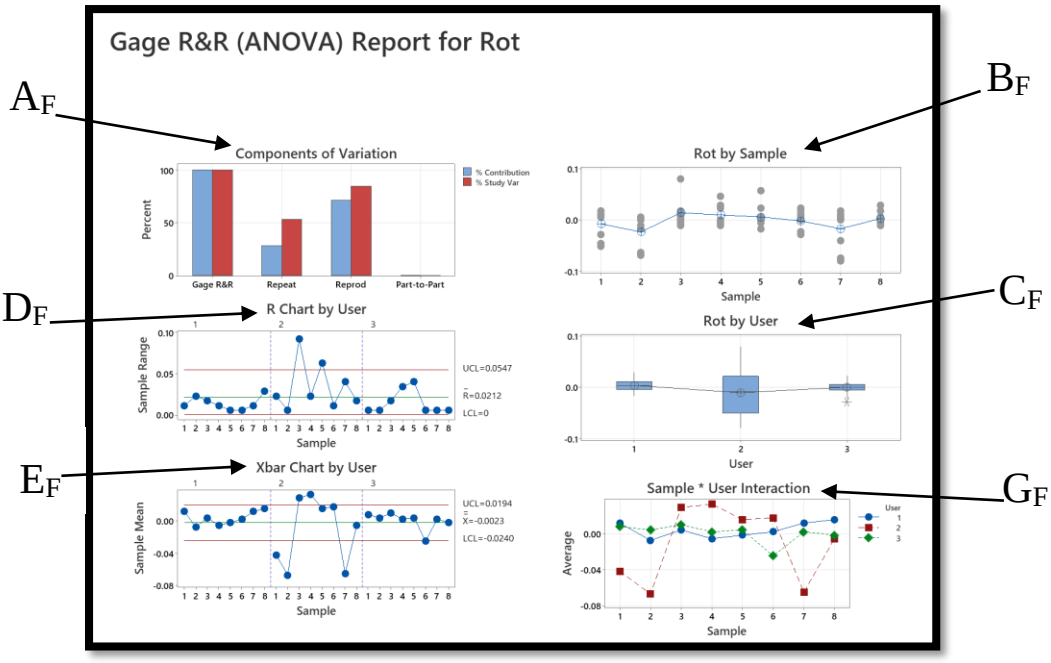

Figure 6.3 Gage R&R for Rot parameter of bones.

A_F This graph represents the percentage differences between Part-Part and Total Gage R&R. If the percent contribution from Part-Part is larger than that of Total Gage R&R, it indicates that most of the variation is attributable to changes between components. If the percent contribution from Total gage R&R is larger than that of Part-To-Part, it means that most of the variation is due to the measuring system (MINITAB 20 support).

B_F The part graph shows whether all the measurements for each part are close together. Multiple measurements for each part that are close together indicating small variation between the measurements of the same part (MINITAB 20 support).

C_F A straight horizontal line across operators is ideally equal amount for each operator. Different measurement average, higher or lower than others, indicates an impact on the final measurement (MINITAB 20 support).

D_F The R chart is a control chart of ranges that shows operator consistency. Any points outside the control limits show inconsistency to the measurement system (MINITAB 20 support).

E_F When most of the points in the Xbar chart are outside the control limits, indicating that the measuring system can identify differences between parts. However, the points inside the control limits of the Xbar mean the variation is mainly due to the measurement system (MINITAB 20 support).

G_F The Operator* Part Interaction graph displays the average measurements by each operator for each part. The parallel line in this graph means there are no interactions. Interactions show that some parts are measured differently by certain operators, which leads to a poor measurement system (MINITAB 20 support).

Based on the brief introduction of Gage R&R charts above, the R chart of Fig. 6.3 depicts the results of each operator's repeated measurements for each part. The control limits of R chart portray a typical range of expected measurement variation. Any data points outside the limits could indicate that the operator or equipment had not consistently measure. As it can be seen from the R chart (Fig 6.3), the data for the other users are between two lines of UCL (Upper control limit) and LCL (Lower control limit), while several data are outside this range for user 2. It can indicate that user 2, measures the part differently than users 1 and 3. This difference is a sign of inconsistency and might be related to inadequate training time or personal inaccuracies of the operator.

The X-bar chart uses the same control limits range of R charts and shows the measurement system variation. In general, for a good measurement system, all points are outside the control limits. This means that the part variation is easy to detect by the measurement system. However, the X-bar chart of users 1 and 3 shows that all data points are inside the control (Fig. 6.3). This indicates that the measuring system is unable to detect part-to-part differences. Due to the large variation of the measurement system, the differences between parts are undetectable.

Moreover, the sample-user interaction chart (Fig. 6.3) shows the patterns of variation for user 2 are different. The absence of parallelism in patterns points to the presence of user-sample interaction. Any interaction is a sign of a poor measurement system and means that parts were measured differently.

The amount of gage R&R from table 6.1 confirms the data plots analysis. The total Gage R&R for Rot samples is 100% which indicates that the measurement system is considered unacceptable (the % Gage R&R is over 30%). This value is obtained from the combination of reproducibility and repeatability. The largest source of variation in this study is related to the appraiser variation. Reproducibility has a percentage of greater than 30% (84.56) which portrays an issue with the operators. Nevertheless, the high level of repeatability (53%) shouldn’t be ignored. Variation in repeatability is conducted to several factors like the equipment and the method of measurement.

Table 6.1 Gage Evaluation of Rot parameter for bone samples.

Source	StdDev (SD)	Study Var (6 × SD)	%Study Var (%SV)
Total Gage R&R	0.0292271	0.175363	**100.00**
Repeatability	0.0156037	0.093622	53.39
Reproducibility	0.0247133	0.148280	84.56
Total Variation	0.0292271	0.175363	100.00

As demonstrated in Fig. 6.4 and Fig 6.5, the influence of the operator on the gauge is also seen in the other two parameters of V/V and F/E.

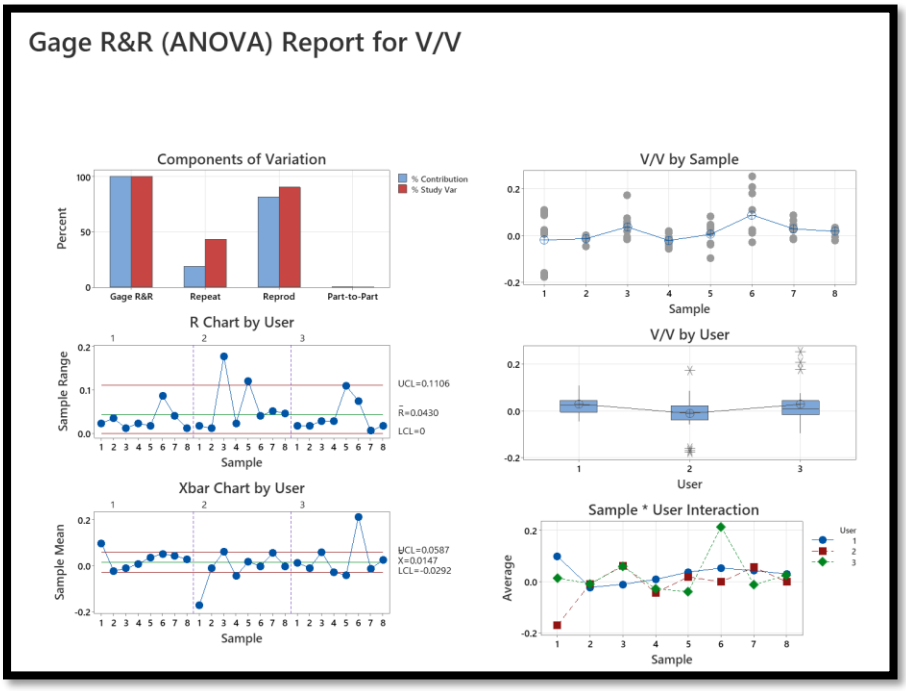

Figure 6.4 Gage R&R for V/V parameter of bones.

For V/V and F/E parameters, patterns of the variation in the sample-user interaction plot are not parallel and different ranges of value are obvious. It can be concluded that the issue is not only related to operator 2. This difference of results by users can be justified by the prob contact force factor. The influence of this factor on the Articulated Arm Coordinate Measuring Machines

(AACMMs) performance has been proven in many studies (Dobosz & Woźniak, 2003; Dobosz & Woźniak, 2005; A Woźniak & Dobosz, 2003; Adam Woźniak & Dobosz, 2005). The manual control of the arm in CMM measuring machines by the operator is a source of non-predictable error. While an operator handles the arm of the CMM, some parameters like contact force and prob orientation effects repeatability and reproducibility values (González-Madruga et al., 2013).

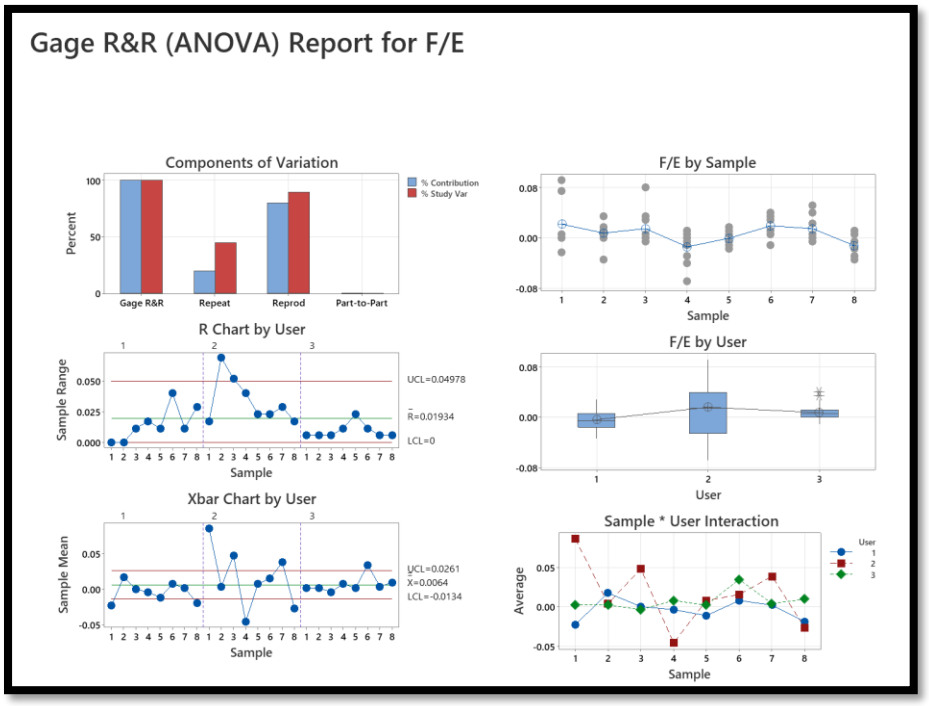

Figure 6.5 Gage R&R for F/E parameter of bones.

6.2.1.1 Gage R&R for Tibial Reference model:

Figures 6.6, 6.7, and 6.8 illustrate the Gage R&R study for results from Tibial Reference samples. Like the Gage study of bones samples, sample-user interaction charts for all 3 three parameters of Rot, V/V, and F/E shows a meaningful difference of results from user 2 and inefficiency of other users. The high level of variation in the measuring system is due to unskilled operators and the high sensitivity of the CMM's running touch. The total gauge R&R for the Rot, V/V, and F/E parameters of TR samples (given in tables 6.2, 6.3, and 6.4) are 100%, 96.53%, and 100% percent, respectively, supporting this conclusion (the accepted criteria is 30%).

Table 6.2 Gage Evaluation of Rot parameter for TR samples.

Source	StdDev (SD)	Study Var (6 × SD)	%Study Var (%SV)
Total Gage R&R	0.0489959	0.293975	**100.00**
Repeatability	0.0378957	0.227374	77.34
Reproducibility	0.0310566	0.186339	63.39
Total Variation	0.0489959	0.293975	100.00

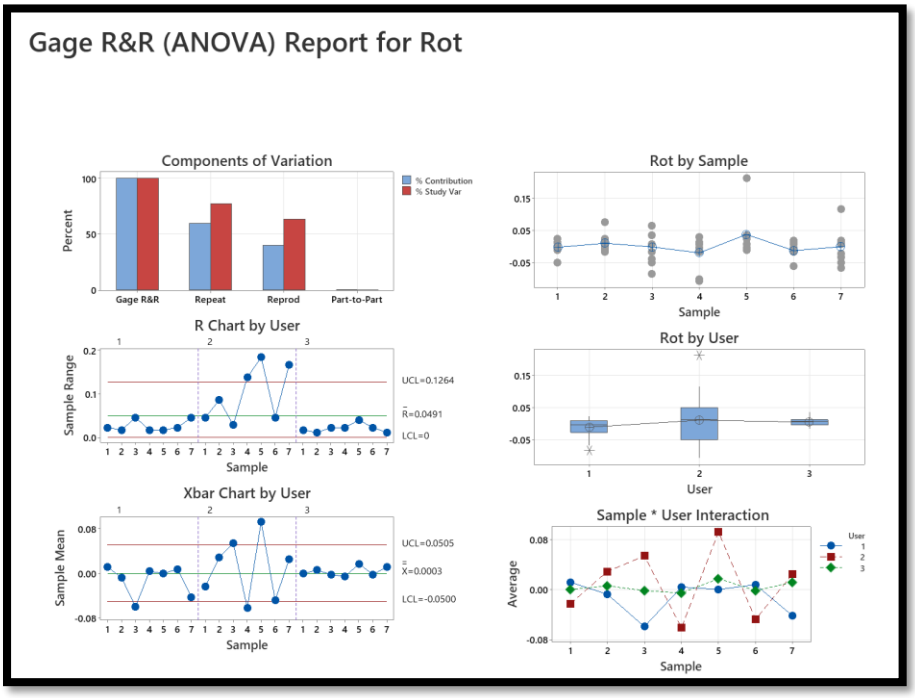

Figure 6.6 Gage R&R for Rot parameter of TR.

Table 6.3 Gage Evaluation of V/V parameter for TR samples.

Source	StdDev (SD)	Study Var (6 × SD)	%Study Var (%SV)
Total Gage R&R	0.0539567	0.323740	**96.53**
Repeatability	0.0406297	0.243778	72.69
Reproducibility	0.0355041	0.213025	63.52
Total Variation	0.0558946	0.335368	100.00

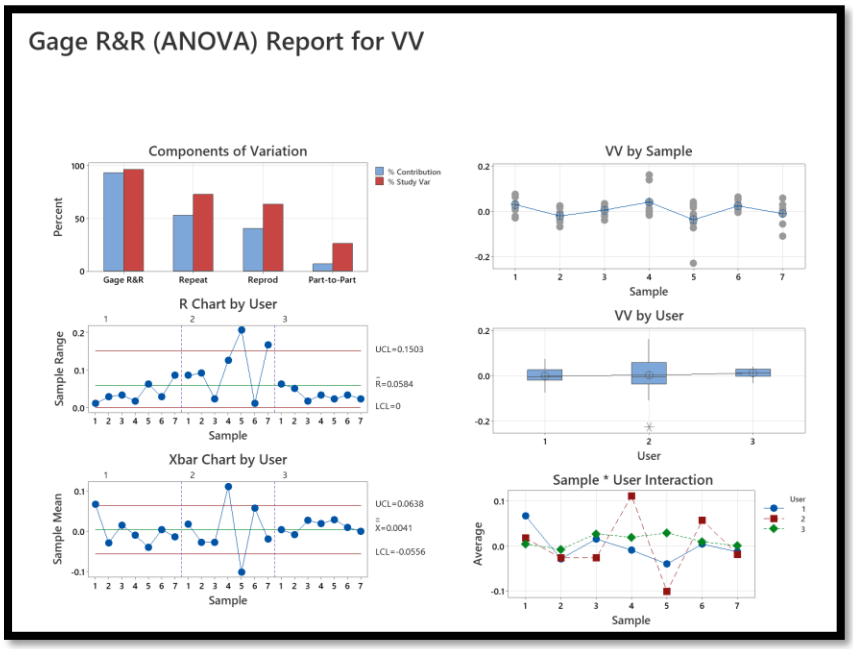

Figure 6.7 Gage R&R for V/V parameter of TR.

Table 6.4 Gage Evaluation of F/E parameter for TR samples.

Source	StdDev (SD)	Study Var (6 × SD)	%Study Var (%SV)
Total Gage R&R	0.0150815	0.0904890	**100.00**
Repeatability	0.0110187	0.0661122	73.06
Reproducibility	0.0102976	0.0617854	68.28
Total Variation	0.0150815	0.0904890	100.00

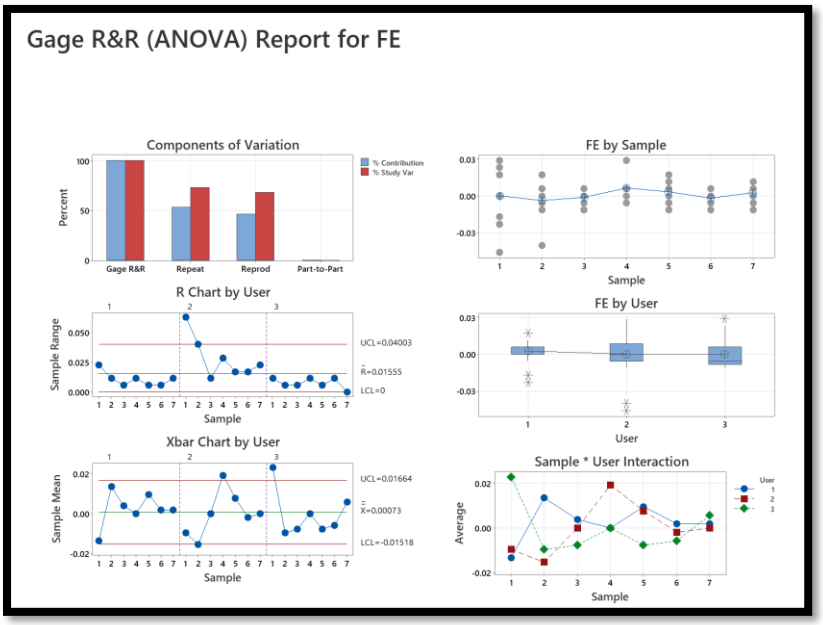

Figure 6.8 Gage R&R for F/E parameter of TR.

Another concern is clamping issues to fix samples on the table. However, all samples are Product Equivalent Units for this test, a 3D printed fixation insert was used to fix the instrument properly to the table to prevent any possible movement between measures. The 3D printed part was designed in accordance with the specification 3D model. The fixation was probably not perfect, and there was thus movement induced between or during acquisitions. Thus, the clamping or location for gaging needs to improve regards to reduce variation.

6.3 Discussion

The Gage R & R study is used to support the measurements of statistical testing and to prove the repeatability and reproducibility of the measurement system. From a Gage study, %EV (the percent the repeatability or equipment variation), %AV (the percent the appraiser variation) and %R&R (The sum of the repeatability and the reproducibility variance components) are calculated.

To sum up the findings, the data results of all the three parameters from bone and TR models are categorized in the following tables (See table 6.5 and 6.6). The %GR&R of all parameters are far away from satisfaction values (higher than the acceptance criteria of 30%) which shows that problems need to be identified and corrected.

Table 6.5 R&R comparison sheet for bone models

R&R comparison sheet of CMM for bone models				
Parameter	Repeatability (%)	Reproducibility (%)	Total %GR&R	
Rot	28.50	71.50	100.00	**>30%**
V/V	18.67	81.33	100.00	**>30%**
F/E	44.86	89.37	100.00	**>30%**

Table 6.6 R&R comparison sheet for TR models.

R&R comparison sheet of CMM for TR models				
Parameter	Repeatability (%)	Reproducibility (%)	Total %GR&R	
Rot	77.34	63.39	100.00	**>30%**
V/V	72.69	63.52	96.53	**>30%**
F/E	73.06	68.28	100.00	**>30%**

Reviewing the highlighted results from the original data, it has been determined that the current measurement system is not sufficient to be conducted to the measuring tasks. As shown in tables 6.5 and 6.6, it has been revealed that the poor capability of the measuring system has resulted from both the measuring device and the operators. In the bone model, the proportion of EV (Repeatability%) values is less than the AV (Reproducibility%) values. This shows the dominating influence of operators on the overall poor capability of the measurement system (See table 6.5). In the TR model, however, both the measuring device and the measuring procedure have a significant impact on the overall low capability (See table 6.6). Therefore, to some extent, the error from the measuring device also could be attributable to improper set-up and poor training for operators.

It is magnificent from this study that as long as the measuring device is a partially manually handheld instrument, the operator is a significant source of variation. Untrained operators have significant impact on the function of instability test for the iASSIST system. Therefore, improved operator training and the use of qualified operators are required. Changes to the measurement system and procedure should be tested until an appropriate solution is found.

CHAPTER 7 CONCLUSION AND RECOMMANDATIONS

7.1 Conclusion

The objective of this test was to characterize the error caused by the instability of the insertion of the Tibial Reference spike into the bone. The instability error results for all 3 parameters, are summarized in table 7.1.

Table 7.1 Rotation, V/V, and F/E instability error results.

Parameter	Instability Error ($\|\mu\| + 3\sigma$)	Measurement Error
Rotation	1.6885°	± 0.964°
Varus/Valgus	1.3179°	± 0.69°
Flexion/Extension	0.6035°	± 1.025°

Based on the ANOVA studies, the repeatability and reproducibility of the measurements with the Faro arm were investigated. All the p-values obtained from ANOVA are greater than the specific value of 0.05, except for the V/V and F/E parameters of the bone model. Therefore, the null hypothesis of ANOVA which assumes that users and samples have different means is rejected. This is a sign of the presence of variation in the measuring system. A gage R&R study was conducted to find out apparent special causes of variations. Both graphical and numerical analysis was applied to estimate the variation and percent of process variation for the total measurement system.

The results from Reproducibility could determine that the operators were a significant source of variation that impacted the variability of the measurement system. Insufficient training time in how to measure the product samples and record the results correctly might be the reason. Furthermore, the great amount of Repeatability shows that a major part of the total variation was related to the gage instrument. This could be justified for two reasons: 1-the high sensitivity of the CMM's running touch, 2- the clamping or location for gaging. Based on the reasons described above, the future research should be conducted to maintain the reliability of the measurement system to ensure the accuracy of the system.

7.2 Recommendations

This chapter offers a series of recommendations to eliminate the issues discovered during test method of measuring system:

7.2.1 An alternative method to FARO arm

The Gage R&R study for Test Method Validation suggests that the Faro CMM method is not feasible as CMM is unable to reach a certain range of reproducibility with touch probes. Therefore, the application of the most recent generation of CMM, like non-contact CMMs could provide the most accurate measurements. Instead of direct contact, these non-contact CMMs rely on lasers, imagery, or sensors technology. In addition, the use of a force sensor might be a helpful alternative. Further studies are needed to evaluate a method with high precision and repeatability.

7.2.2 Development of a Cause-and-Effect Diagram

Analyzing whether the error of measurement system comes from the process, or the measurement device helps to save resources, time, and corrective actions can be taken. To find out the solution, constructing a Cause-and-Effect Diagram could be a beneficial tool to recognize, sort, and show the quality characteristic of the problem. The diagrams obtained from this method, illustrate the relationship between the factors that influence the outcomes.

BIBLIOGRAPHY

Abulhasan, J. F., Grey, M. J. J. J. o. F. M., & kinesiology. (2017). Anatomy and physiology of knee stability. *2*(4), 34.

THE ATTUNE CEMENTLESs KNEE SYSTEM. Retrieved from https://www.attuneevidence.com/additional-information

Azar, F. M., Canale, S. T., & Beaty, J. H. (2020). *Campbell's Operative Orthopaedics, E-Book*: Elsevier Health Sciences.

Babazadeh, S., Stoney, J. D., Lim, K., & Choong, P. F. J. O. r. (2009). The relevance of ligament balancing in total knee arthroplasty: how important is it? A systematic review of the literature. *1*(2).

Badley, E., Wilfong, J., Zahid, S., & Perruccio, A. J. A. f. t. A. S. (2019). The status of arthritis in Canada: national report.

Badley, E. D., M. (2003). Arthritis in Canada: An Ongoing Challenge. Ottawa:

Health Canada.

.

biomet, Z. (2016). NexGen®CR-Flex and LPS-Flex Knees. file:///C:/Users/asras/Downloads/nexgen-cr-flex-and-lps-flex-knees-design-rationale.pdf

Blankstein, A. R., Houston, B. L., Fergusson, D. A., Houston, D. S., Rimmer, E., Bohm, E., . . . Open, J. (2021). Transfusion in orthopaedic surgery: a retrospective multicentre cohort study. *2*(10), 850-857.

Browne, J. A., Cook, C., Hofmann, A. A., & Bolognesi, M. P. J. T. K. (2010). Postoperative morbidity and mortality following total knee arthroplasty with computer navigation. *17*(2), 152-156.

code of Federal regulation. (2022).

Concoff, A., Niazi, F., Farrokhyar, F., Alyass, A., Rosen, J., Nicholls, M. J. C. M. I. A., & Disorders, M. (2021). Delay to TKA and Costs Associated with Knee Osteoarthritis Care Using Intra-Articular Hyaluronic Acid: Analysis of an Administrative Database. *14*, 11795441211994092.

Daines, B. K., & Dennis, D. A. J. C. i. o. s. (2014). Gap balancing vs. measured resection technique in total knee arthroplasty. *6*(1), 1-8.

Dennis, D. A., Komistek, R. D., Mahfouz, M. R., Walker, S. A., Tucker, A. J. C. O., & Research, R. (2004). A multicenter analysis of axial femorotibial rotation after total knee arthroplasty. *428*, 180-189.

Dobosz, M., & Woźniak, A. J. M. (2003). Metrological feasibilities of CMM touch trigger probes: Part II: Experimental verification of the 3D theoretical model of probe pretravel. *34*(4), 287-299.

Dobosz, M., & Woźniak, A. J. P. E. (2005). CMM touch trigger probes testing using a reference axis. *29*(3), 281-289.

Edwards, A., Bull, A. M., Amis, A. A. J. A. T. J. o. A., & Surgery, R. (2007). The attachments of the fiber bundles of the posterior cruciate ligament: an anatomic study. *23*(3), 284-290.

Feeley, B. T., Gallo, R. A., Sherman, S., & Williams, R. J. J. J.-J. o. t. A. A. o. O. S. (2010). Management of osteoarthritis of the knee in the active patient. *18*(7), 406-416.

Figueroa, F., Parker, D., Fritsch, B., Oussedik, S. J. J. o. I. J. D., & Medicine, O. S. (2018). New and evolving technologies for knee arthroplasty—computer navigation and robotics: state of the art. *3*(1), 46-54.

Fitness, R. H. (2019). Conditioning for ACL Injury Prevention. Retrieved from https://reversagehealthandfitness.com/2018/12/09/conditioning-for-acl-injury-prevention/?msclkid=e86823d3a92611ec8958a263244e50c9

Freeman, M., Swanson, S., Todd, R. J. C. O., & Research, R. (1973). Total replacement of the knee using the Freeman-Swanson knee prosthesis. *94*, 153-170.

Goh, G. S.-H., Liow, M. H. L., Lim, W. S.-R., Tay, D. K.-J., Yeo, S. J., & Tan, M. H. J. T. J. o. a. (2016). Accelerometer-based navigation is as accurate as optical computer navigation in restoring the joint line and mechanical axis after total knee arthroplasty: a prospective matched study. *31*(1), 92-97.

González-Madruga, D., Cuesta, E., Barreiro, J., & Fernandez-Abia, A. I. J. S. (2013). Application of a force sensor to improve the reliability of measurement with articulated arm coordinate measuring machines. *13*(8), 10430-10448.

Howell, S., & Hull, M. J. A. (2014). Kinematic alignment in total knee arthroplasty. Definition, history, principle, surgical technique, and results of an alignment option for TKA. *1*, 44-53.

Insall, J. N. (1993). Surgical techniques and instrumentation in total knee arthroplasty.

Insall, J. N., Binazzi, R., Soudry, M., Mestriner, L. A. J. C. o., & research, r. (1985). Total knee arthroplasty. (192), 13-22.

Insall, J. N., Scuderi, G. R., Komistek, R. D., Math, K., Dennis, D. A., & Anderson, D. T. (2002). Correlation Between Condylar Lift-Off and Femoral Component Alignment. *403*, 143-152.

Iseki, Y., Takahashi, T., Takeda, H., Tsuboi, I., Imai, H., Mashima, N., . . . cartilage. (2009). Defining the load bearing axis of the lower extremity obtained from anterior-posterior digital radiographs of the whole limb in stance. *17*(5), 586-591.

Jacofsky, D. J. A. (2016). Robotics in arthroplasty: a comprehensive review. *31*(10), 2353-2363.

Jacofsky, D. J. A. (2016). Robotics in Arthroplasty: A Comprehensive Review. *31 10*, 2353-2363.

JC, T. J. S. E. P. (2010). Netter's concise orthopaedic anatomy. 30-31.

Johan Bellemans, M., Colyn, W., Vandenneucker, H., Jan Victor, M. J. C. O., & Research, R. (2012). The Chitranjan Ranawat Award: Is Neutral Mechanical Alignment Normal for All Patients?: The Concept of Constitutional Varus. *470*(1), 45.

Jones, C. W., & Jerabek, S. A. J. T. J. o. a. (2018). Current role of computer navigation in total knee arthroplasty. *33*(7), 1989-1993.

Kang, K.-T., Koh, Y.-G., Son, J., Kwon, O.-R., Lee, J.-S., & Kwon, S.-K. J. T. J. o. a. (2018). Influence of increased posterior tibial slope in total knee arthroplasty on knee joint biomechanics: a computational simulation study. *33*(2), 572-579.

Kazerouni, A. M. J. W. A. o. S., Engineering, Technology, I. J. o. M., Aerospace, Industrial, Mechatronic, & Engineering, M. (2009). Design and Analysis of Gauge R&R Studies: Making Decisions Based on ANOVA Method. *3*, 335-339.

Kinney, M. C., Cidambi, K. R., Severns, D. L., & Gonzales, F. B. J. T. J. o. a. (2018). Comparison of the iAssist handheld guidance system to conventional instruments for mechanical axis restoration in total knee arthroplasty. *33*(1), 61-66.

Lanting, B. A., Williams, H. A., Matlovich, N. F., Vandekerckhove, P.-J., Teeter, M. G., Vasarhelyi, E. M., . . . Somerville, L. E. J. T. K. (2018). The impact of residual varus alignment following total knee arthroplasty on patient outcome scores in a constitutional varus population. *25*(6), 1278-1282.

Le, D. H., Goodman, S. B., Maloney, W. J., Huddleston, J. I. J. C. O., & Research®, R. (2014). Current modes of failure in TKA: infection, instability, and stiffness predominate. *472*(7), 2197-2200.

Li, J. t., Gao, X., & Li, X. J. O. s. (2019). Comparison of iASSIST Navigation System with Conventional Techniques in Total Knee Arthroplasty: A Systematic Review and Meta-Analysis of Radiographic and Clinical Outcomes. *11*(6), 985-993.

Luo, Z., Zhou, K., Peng, L., Shang, Q., Pei, F., & Zhou, Z. (2020). Similar results with kinematic and mechanical alignment applied in total knee arthroplasty. *Knee Surgery, Sports Traumatology, Arthroscopy*, *28*(6), 1720-1735. doi:10.1007/s00167-019-05584-2

Mathers, C. D., & Loncar, D. J. P. m. (2006). Projections of global mortality and burden of disease from 2002 to 2030. *3*(11), e442.

Matsuzaki, T., Matsumoto, T., Kubo, S., Muratsu, H., Matsushita, T., Kawakami, Y., . . . Kurosaka, M. J. K. S., Sports Traumatology, Arthroscopy. (2014). Tibial internal rotation is affected by lateral laxity in cruciate-retaining total knee arthroplasty: an intraoperative kinematic study using a navigation system and offset-type tensor. *22*(3), 615-620.

Mattei, L., Pellegrino, P., Calò, M., Bistolfi, A., & Castoldi, F. J. A. o. t. m. (2016). Patient specific instrumentation in total knee arthroplasty: a state of the art. *4*(7).

Nam, D., McArthur, B. A., Cross, M. B., Pearle, A. D., Mayman, D. J., & Haas, S. B. J. T. j. o. k. s. (2012). Patient-specific instrumentation in total knee arthroplasty: a review. *25*(03), 213-220.

Nam, D., Nunley, R. M., & Barrack, R. L. (2014). Patient dissatisfaction following total knee replacement: a growing concern? *Bone Joint J, 96-b*(11 Supple A), 96-100. doi:10.1302/0301-620x.96b11.34152

Nam, D., Weeks, K. D., Reinhardt, K. R., Nawabi, D. H., Cross, M. B., & Mayman, D. J. J. T. J. o. a. (2013). Accelerometer-based, portable navigation vs imageless, large-console

computer-assisted navigation in total knee arthroplasty: a comparison of radiographic results. *28*(2), 255-261.

National Joint Replacement Registry AOA Hip. (2021). Knee & Shoulder Arthroplasty 2020 Annu

Rep 2020

National Joint Replacement Registry AOA Hip, Knee & Shoulder Arthroplasty (2020). *2020 Annu*

Rep, 244.

Oga, Y., Tomonari, H., Kwon, S., Kuninori, T., Yagi, T., & Miyawaki, S. J. T. A. O. (2019). Evaluation of miniscrew stability using an automatic embedding auxiliary skeletal anchorage device. *89*(1), 47-53.

Pailhé, R. J. O., Surgery, T., & Research. (2021). Total knee arthroplasty: latest robotics implantation techniques. *107*(1), 102780.

Parcells, B. W., & Tria Jr, A. J. J. A. J. O. (2016). The cruciate ligaments in total knee arthroplasty. *45*(4), 153-160.

Picard, F., Deep, K., & Jenny, J. Y. J. K. S., Sports Traumatology, Arthroscopy. (2016). Current state of the art in total knee arthroplasty computer navigation. *24*(11), 3565-3574.

Picard, F., Gregori, A., Leitner, F., Saragaglia, D., & DiGioia, A. M. (2007). *Computer assisted orthopaedics: the image free concept*: Pro Business.

Plaskos, C., Hodgson, A. J., Inkpen, K., & McGraw, R. W. J. T. J. o. a. (2002). Bone cutting errors in total knee arthroplasty. *17*(6), 698-705.

Pros & Cons of Robotic-Assisted Surgery. (2014). Retrieved from https://www.globalpremeds.com/2014/02/12/pros-cons-of-robotic-assisted-surgery/?msclkid=58522e05a93811ecbe7d00f7b8eccadd

Quack, V. M., Kathrein, S., Rath, B., Tingart, M., & Lüring, C. (2012). Computer-assisted navigation in total knee arthroplasty: a review of literature. *Biomed Tech (Berl), 57*(4), 269-275. doi:10.1515/bmt-2011-0096

ROSA Knee System. (2022). Retrieved from https://www.zimmerbiomet.com/en/products-and-solutions/specialties/knee/rosa--knee-system.html?msclkid=a884098da93c11eca9e55f72879fad2e

Schiraldi, M., Bonzanini, G., Chirillo, D., & de Tullio, V. J. A. o. t. m. (2016). Mechanical and kinematic alignment in total knee arthroplasty. *4*(7).

Schneider, O., & Troccaz, J. J. C. a. s. (2001). A six-degree-of-freedom passive arm with dynamic constraints (PADyC) for cardiac surgery application: Preliminary experiments. *6*(6), 340-351.

Sharkey, P., Hozack, W., Rothman, R., Shastri, S., & Jacoby, S. J. C. O. R. R. (2002). Why are total knee arthroplasties failing today? Insall Award Paper. *404*, 7-13.

Sheth, N. P., Husain, A., & Nelson, C. L. (2017). Surgical Techniques for Total Knee Arthroplasty: Measured Resection, Gap Balancing, and Hybrid. *J Am Acad Orthop Surg, 25*(7), 499-508. doi:10.5435/jaaos-d-14-00320

Sheth, N. P., Husain, A., & Nelson, C. L. J. J.-J. o. t. A. A. o. O. S. (2017). Surgical techniques for total knee arthroplasty: measured resection, gap balancing, and hybrid. *25*(7), 499-508.

Siston, R. A., Giori, N. J., Goodman, S. B., & Delp, S. L. J. J. o. b. (2007). Surgical navigation for total knee arthroplasty: a perspective. *40*(4), 728-735.

Smith & Nephew Launches NAVIO for Total Knee. (2017). Retrieved from https://www.innovahealthpartners.com/interests/smith-nephew-launches-navio-total-knee/?msclkid=f5eecfbda93a11ec90fd5d820f99ec80

Solution, N. C. K. J. I. (1995). Intramedullary Instrumentation Surgical Technique, For The NexGen Cruciate Retaining & Legacy Posterior Stabilized Knee, Zimmer. *1997*, 1998.

Stiehl, J. B., DiGioia, A. M., Haaker, R. G., & Konermann, W. H. (2007). *Navigation and MIS in orthopedic surgery*: Springer.

Stryker. (2007a). precisioN Knee Navigation Operative Technique.

Stryker. (2007b). precisioN Knee Navigation Operative Technique for precisioN Knee Software, Literature No.

Stryker celebrates 1,000th install of Mako System. (2020). Retrieved from https://www.surgicalroboticstechnology.com/news/stryker-celebrates-1000th-install-of-mako-system/?msclkid=6afaa8b9a93a11ecb75c59b7845eb5f5

Sugano. (2003). Computer-assisted orthopedic surgery. *8*(3), 442-448.

Surgeons, A. A. o. O. (2021). Total Knee Replacement. Retrieved from https://orthoinfo.aaos.org/en/treatment/total-knee-replacement?msclkid=3f990e80a92211ec82c09043f72751ff

Tapasvi, S. R., Shekhar, A., Patil, S. S., Dipane, M. V., Chowdhry, M., & McPherson, E. J. J. T. J. o. a. (2020). Comparison of gap balancing vs measured resection technique in patients undergoing simultaneous bilateral total knee arthroplasty: one technique per knee. *35*(3), 732-740.

Thomas Parker Vail, J. E. L., C. Van Sikes, III. (2016). Surgical Techniques and Instrumentation in Total Knee Arthroplasty. Retrieved from https://musculoskeletalkey.com/surgical-techniques-and-instrumentation-in-total-knee-arthroplasty-2/?msclkid=df5d9969a92a11ec991a47662c015921

Vandekerckhove, P.-J. T., Matlovich, N., Teeter, M. G., MacDonald, S. J., Howard, J. L., & Lanting, B. A. J. K. S., Sports Traumatology, Arthroscopy. (2017). The relationship between constitutional alignment and varus osteoarthritis of the knee. *25*(9), 2873-2879.

Whitaker, A. T., & Vuillermin, C. J. C. r. i. m. m. (2016). Lower extremity growth and deformity. *9*(4), 454-461.

Whitesides, T. E. (2001). Orthopaedic basic Science. Biology and biomechanics of the musculoskeletal system. In: LWW.

Woźniak, A., & Dobosz, M. J. M. (2003). Metrological feasibilities of CMM touch trigger probes. Part I: 3D theoretical model of probe pretravel. *34*(4), 273-286.

Woźniak, A., & Dobosz, M. J. P. E. (2005). Influence of measured objects parameters on CMM touch trigger probe accuracy of probing. *29*(3), 290-297.

Younger, A., Wing, K., Penner, M., & Cresswell, M. J. K. S., Sports Traumatology, Arthroscopy. (2016). A study to evaluate the safety of platelet-derived growth factor for treatment of osteochondral defects of the talus. *24*(4), 1250-1258.

Zhang, Y., & Jordan, J. M. J. C. i. g. m. (2010). Epidemiology of osteoarthritis. *26*(3), 355-369.